arXiv:2610.14511v2 [econ.EM] 25 Oct 2026

A Balanced Parametrization of Correlation Matrices*

Peter Reinhard Hansen§ and Chen Tong‡

§Department of Economics, University of North Carolina at Chapel Hill

‡School of Economics, Xiamen University

October 2026

Abstract

We introduce the *balanced correlation parametrization* (BCP), which maps positive-definite correlation matrices one-to-one onto the set of symmetric hollow (zero-diagonal) matrices with unrestricted off-diagonal entries. A key feature of the parametrization is that both the transformation and its inverse are available in closed form. It can be viewed as a generalization of the transformation underlying the classical correlation t-statistic to higher dimensions. It has a direct interpretation as a scaled sum of marginal and partial correlations, is inverse-consistent and equivariant under variable permutations and sign changes, and preserves block structure. A novel property of BCP is that it preserves correlation sparsity as the dimension tends to infinity under suitable factor conditions, providing a basis for sparse high-dimensional correlation modeling. An empirical illustration using standardized idiosyncratic daily stock returns for 1,765 equities over 15 years shows that BCP retains the approximate sparsity pattern and magnitudes of shock correlations, and that it yields accurate positive-definite reconstructions under sparse coordinate restrictions.

Keywords: correlation matrix; unconstrained parametrization; balanced correlation parametrization; asymptotic sparsity; high-dimensional correlation

MSC 2020: 15B48; 15A16; 15A24; 53B20; 62H20

*Corresponding author: Peter Reinhard Hansen. Email: hansen@unc.edu. Chen Tong acknowledges financial support from the National Natural Science Foundation of China (72301227, 72673150) and the Fujian Provincial Natural Science Foundation of China (2025J08008).

1 Introduction

Correlation matrices are central to multivariate models in statistics, econometrics, and finance. They enter likelihoods, copula models, and the analysis of portfolio risk.[1] Positive definiteness constrains the individual correlation coefficients, which prevents their use as unrestricted parameters.[2] Covariance normalization, as in the DCC model of Engle (2002), rescales an auxiliary positive-definite matrix to unit diagonal. However, this matrix is not uniquely identified, since positive diagonal rescalings leave its correlations unchanged.

The literature has introduced several one-to-one parametrizations that avoid both problems. These include Cholesky and modified Cholesky factorizations (Pinheiro & Bates, 1996; Pourahmadi, 1999; van Oest, 2021; Thanwerdas & Pennec, 2022), spherical coordinates (Rapisarda et al., 2007; Pourahmadi & Wang, 2015; Tsay & Pourahmadi, 2017; Forrester & Zhang, 2020; Lucchetti & Pedini, 2024), and sequential or vine-based partial correlations (Kurowicka & Cooke, 2003; Joe, 2006; Daniels & Pourahmadi, 2009; Lewandowski et al., 2009; Sturmfels et al., 2016). These constructions provide explicit, computationally convenient coordinates that can be transformed componentwise into unrestricted real parameters. However, the coordinates depend on the ordering of the variables. Matrix-logarithmic covariance models avoid this dependence (Leonard & Hsu, 1992; Chiu et al., 1996). However, the matrix logarithms of correlation matrices do not fill a linear space, because their diagonal entries are constrained by the unit-diagonal normalization.

Archakov & Hansen (2021) overcome this problem by retaining the off-diagonal entries of the matrix logarithm. Their generalized Fisher transformation (GFT) is a global parametrization that does not depend on variable ordering. Zwiernik (2025) applies the same idea to the inverse correlation matrix, whose off-diagonal entries give another unrestricted parametrization (InvC). However, inversion of both GFT and InvC requires a numerically determined diagonal correction. The log-scaling (LS) transformation of Thanwerdas (2024) has a direct inverse and treats normalized correlation inversion symmetrically, but its transformation from correlation matrices to the LS coordinates is not in closed form.

In this paper, we introduce the balanced correlation parametrization (BCP), which maps positive-definite correlation matrices one-to-one onto symmetric hollow (zero-diagonal) matrices with unrestricted off-diagonal entries. This means that positive-definite correlation matrices can be parametrized by an unrestricted vector in $\mathbb{R}^{n(n-1)/2}$, as is the case for GFT,

[1] Examples include multivariate GARCH models with dynamic correlations (Engle, 2002; Tse & Tsui, 2002; Creal et al., 2011; Engle & Kelly, 2012; Aielli, 2013; Engle et al., 2019; Pakel et al., 2021; Archakov et al., 2026; Tong et al., 2026; Tong & Hansen, 2026) and dynamic copula models with time-varying correlations (Creal & Tsay, 2015; Oh & Patton, 2018, 2023; Opschoor et al., 2021; Hafner & Wang, 2023).

[2] The constraints are severe in high dimensions, where valid correlation matrices occupy a vanishing fraction of the cube of entries, see Böhm & Hornik (2014) and Hansen (2026).

InvC, and LS. For a positive-definite correlation matrix C, the transformation $B(C)$ and its inverse are given by

$$B(C) = \tfrac{1}{2}\left(D^{1/4} C D^{1/4} - D^{-1/4} C^{-1} D^{-1/4}\right),$$
$$C(B) = \mathrm{Cor}(B + \sqrt{I_n + B^2}),$$

where $D = \mathrm{Diag}(C^{-1})$ is the diagonal part of C^{-1}, and $\mathrm{Cor}(\Sigma) = \mathrm{Diag}(\Sigma)^{-1/2}\Sigma\,\mathrm{Diag}(\Sigma)^{-1/2}$ rescales a positive-definite symmetric matrix to have unit diagonal. The key advantage of BCP over GFT, InvC, and LS is that both the transformation and its inverse are available in closed form and require no iterative scaling or diagonal completion. Moreover, BCP has a range of additional convenient properties, including: explicit derivatives, which support estimation and likelihood optimization; equivariance under variable permutations and sign changes; inverse consistency; exact preservation of block structure; and interpretable coordinates that combine marginal and partial correlations. A novel property of BCP is that it preserves correlation sparsity as the dimension tends to infinity under suitable factor conditions, providing a basis for sparse high-dimensional correlation modeling. The other parametrizations share some of these properties, as summarized in Table 1.

In the bivariate case, applying BCP to the sample correlation yields exactly the classical t-statistic up to a sample-size scaling factor. Let $\hat{\rho}$ denote the sample correlation from T i.i.d. bivariate Gaussian observations. Under the null hypothesis of zero correlation,

$$\frac{\hat{\rho}}{\sqrt{1-\hat{\rho}^2}} \sim t_{T-2}\left(0, \frac{1}{T-2}\right), \qquad \mathrm{atanh}(\hat{\rho}) \overset{a}{\sim} N\left(0, \frac{1}{T-3}\right).$$

The first transformation is the bivariate BCP, and the second is Fisher's z-transformation. The parametrization of Archakov & Hansen (2021) recovers this transformation in the bivariate case, hence the name generalized Fisher transformation. Like GFT, BCP extends a familiar scalar transformation from classical correlation inference to the multivariate setting, providing an unrestricted parametrization of correlation matrices.

The term *balanced* refers to the balancing condition underlying BCP's one-to-one mapping from the set $\mathcal{C}_n$ of $n \times n$ positive-definite correlation matrices onto the space $\mathbb{H}_n$ of symmetric hollow matrices. The construction uses the fact that positive diagonal rescaling leaves correlations unchanged. With $D = \mathrm{Diag}(C^{-1})$, the matrix $D^{1/4}$ is the unique positive diagonal scaling for which $A = D^{1/4} C D^{1/4}$ and A^{-1} have the same diagonal. This condition makes $B(C) = \frac{1}{2}(A - A^{-1})$ hollow, while $B + \sqrt{I_n + B^2}$ is positive definite for every symmetric B and yields a correlation matrix after normalization. The resulting coordinates also have a statistical interpretation. Write $K = C^{-1}$, let $\pi_{ij} = -K_{ij}/\sqrt{K_{ii}K_{jj}}$ be the full partial correlation, and

let $\tau_i = K_{ii}^{-1/2}$ be the residual standard deviation from projecting standardized variable i on all the other variables. Each coordinate combines marginal and partial correlations, scaled by the residual risk of the two variables:

$$[B(C)]_{ij} = \frac{C_{ij} + \pi_{ij}}{2\sqrt{\tau_i \tau_j}}, \qquad i \neq j.$$

The main contribution of the paper is to introduce BCP, establish that it is a global real-analytic bijection, and characterize its construction through a rigidity theorem. Choosing the diagonal scale before applying the spectral transformation makes the complete image hollow, so inversion requires no recovery of an omitted diagonal. For $n \geq 3$, direct hollowness and unit local normalization uniquely determine BCP among primary spectral transformations of balanced representatives (Theorem 2). Block symmetry becomes linear restrictions on the transformed entries and permits computation at the block level. Exact preservation also yields a new unrestricted parametrization of block correlation matrices, providing an alternative to the GFT-based parametrization discussed by Tong & Hansen (2023). We also derive simplified BCP expressions for arrowhead, Gaussian-tree, moving-average, autoregressive, and factor-model correlation matrices (Section 6), together with explicit derivatives and a closed-form Jacobian determinant for likelihood optimization, inference, and density transformation.

The literature on parametrization and sparsity emphasizes that zero patterns and their interpretation depend on the scale used to represent dependence (Battey, 2017, 2019; Rybak & Battey, 2021; Rybak et al., 2026). Related algebraic properties of logarithmic sparsity are studied by Pavlov (2024). Saxena et al. (2023) and Huang et al. (2025) develop Cholesky-based methods for imposing specified correlation zeros. However, both depend on variable ordering and require parameter adjustments tailored to the zero pattern. We show that, under suitable factor conditions, BCP preserves marginal-correlation sparsity as the dimension tends to infinity: a coordinate tends to zero if and only if its corresponding correlation does. Each coordinate is a positively rescaled correlation up to a uniform error of order μ_n^{-1}, where μ_n is the strength of the weakest factor direction relative to residual noise. A common magnitude threshold can therefore recover the entire marginal-correlation support under suitable signal and estimation-error conditions. Under the same factor conditions, all GFT and InvC coordinates shrink uniformly at rates $O(\log(1 + \mu_n)/\mu_n)$ and $O(\mu_n^{-1})$, respectively. GFT, InvC, and LS do not share BCP's general support-recovery guarantee: a zero correlation can produce a larger coordinate magnitude than a fixed nonzero correlation, even after common rescaling. For a bounded number of factors, zeroing BCP coordinates at population correlation zeros also yields a positive-definite reconstruction whose maximum entrywise error tends to zero. These results provide a basis for sparse high-dimensional

correlation modeling in unrestricted coordinates, although exact entrywise zeros need not be preserved at finite dimension.

Our empirical illustration uses a high-dimensional balanced panel of idiosyncratic daily stock returns for 1,765 equities over the 15-year period 2011–2025. We remove the Fama–French five factors and momentum from each stock's daily return and fit a univariate GJR-GARCH model to the residuals. We compare the correlations of the resulting standardized shocks with their BCP, GFT, LS, and InvC coordinates. BCP retains the visible approximate sparsity pattern, sector structure, and entry magnitudes of shock correlations, whereas the alternative coordinates track marginal correlations less directly. The smoothed conditional-coordinate plots support this comparison: the BCP median tracks shock correlations more closely, while GFT and LS medians remain closer to zero and the InvC median slopes downward. We also impose a common zero pattern selected by pointwise 5% correlation significance tests. For this sample and these restrictions, BCP yields a positive-definite estimate that more closely tracks both the original and directly thresholded correlations and has a lower descriptive BIC than GFT, LS, or InvC. These findings illustrate how BCP accommodates sparse coordinate restrictions while yielding a positive-definite reconstruction that closely approximates the original correlation matrix.

The paper is organized as follows. Section 2 introduces the notation, then constructs and characterizes BCP. Section 3 establishes its structural properties. Section 4 presents differentiation, inference, and the local relation to GFT. Section 5 develops reduced block formulas, and Section 6 gives explicit BCP expressions for selected structured families. Building on the factor-model formulas, Section 7 establishes asymptotic sparsity preservation and compares GFT, InvC, and LS. Section 8 presents the standardized-shock illustration. The separate supplement contains proofs, extensions, and computational details. Its sections, equations, and tables carry an S prefix.

2 Construction and characterization of BCP

We construct BCP in two steps. First, we select a unique positive diagonal rescaling of each correlation matrix whose diagonal matches that of its inverse. We then characterize the spectral transformation that maps these balanced matrices to hollow matrices. The resulting transformation and its inverse are explicit.

Table 1: Comparison of properties of correlation-matrix parametrizations.

Method	Closed form both ways	Permutation-equivariant	Sign-equivariant	Inverse-consistent	Preserves Block	Asymptotic Sparsity
Partial correlation[†]	Yes	No	Yes	No	No	No
GFT	No	Yes	Yes	No	Yes	No
InvC	No	Yes	Yes	No	Yes	No
LS	No	Yes	No	Yes	Yes	No
BCP	**Yes**	**Yes**	**Yes**	**Yes**	**Yes**	**Yes**

Notes: [†]Fixed-order partial-correlation, Cholesky, and hyperspherical parametrizations in sign-equivariant unrestricted coordinates. Inverse consistency: C and $\mathcal{I}(C)$ have opposite coordinates. Preserves block: block structure is preserved in both directions. Asymptotic sparsity: under the conditions of Theorem 10, a coordinate vanishes if and only if the corresponding correlation does as $n \to \infty$; exact zeros need not be preserved at finite n. "No" means not in general.

2.1 Notation and preliminaries

Let I_n be the $n \times n$ identity matrix and $\mathbb{S}_n$ the vector space of symmetric $n \times n$ matrices, with symmetric positive-definite (SPD) cone $\mathbb{S}_n^{++}$. Write $\mathcal{C}_n = \{C \in \mathbb{S}_n^{++} : \mathrm{Diag}(C) = I_n\}$ for the set of positive-definite correlation matrices and $\mathbb{H}_n = \{X \in \mathbb{S}_n : \mathrm{Diag}(X) = 0\}$ for the symmetric hollow matrices. Both spaces have dimension $d = n(n-1)/2$. For a matrix X and vector x, $\mathrm{diag}(X)$ extracts the diagonal vector, $\mathrm{diag}(x)$ forms a diagonal matrix, and $\mathrm{Diag}(X) = \mathrm{diag}\{\mathrm{diag}(X)\}$.

For symmetric X, the projection onto $\mathbb{H}_n$ is $\mathrm{Off}(X) = X - \mathrm{Diag}(X)$. We use $\mathrm{tr}(X)$, $\|X\|_2$, and $\|X\|_F$ for the trace, spectral norm, and Frobenius norm, respectively, and ι_n for the n-vector of ones, omitting its subscript when dimension is clear.

For $\Sigma \in \mathbb{S}_n^{++}$, correlation normalization $\mathrm{Cor}(\Sigma) = \mathrm{Diag}(\Sigma)^{-1/2}\Sigma\,\mathrm{Diag}(\Sigma)^{-1/2}$ maps a covariance matrix to the corresponding correlation matrix. The *normalized correlation inverse* $\mathcal{I}(C) = \mathrm{Cor}(C^{-1})$ gives the full partial correlations $\pi_{ij} = -[\mathcal{I}(C)]_{ij} = -K_{ij}/\sqrt{K_{ii}K_{jj}}$, $i \neq j$, where $K = C^{-1}$. A transformation Φ is *inverse-consistent* if $\Phi\{\mathcal{I}(C)\} = -\Phi(C)$. The signed permutation group $\mathfrak{S}_n^{\pm}$ consists of matrices $Q = EP$, where P is a permutation matrix and $E = \mathrm{diag}(\varepsilon_1, \ldots, \varepsilon_n)$, $\varepsilon_i \in \{-1, 1\}$.

2.2 The balanced representative

For each $C \in \mathcal{C}_n$, we seek a positive-definite representative A_C satisfying $\mathrm{Cor}(A_C) = C$ and a scalar spectral transformation g such that

$$B = g(A_C) \in \mathbb{H}_n, \qquad C = \mathrm{Cor}\big(g^{-1}(B)\big) \in \mathcal{C}_n.$$

Every such representative has the form $A = \Delta C \Delta$ for a positive diagonal matrix Δ. We select the scale by requiring the matrix and its inverse to have the same diagonal, a condition preserved by inversion.

Definition 1 (Balanced matrices)**.** A symmetric positive-definite matrix $A \in \mathbb{S}_n^{++}$ is *balanced* if its diagonal equals that of its inverse,

$$\mathrm{Diag}(A) = \mathrm{Diag}(A^{-1}). \tag{1}$$

The set of balanced $n \times n$ matrices is $\mathbb{B}_n = \{A \in \mathbb{S}_n^{++} : \mathrm{Diag}(A) = \mathrm{Diag}(A^{-1})\}$.

Theorem 1 (Unique balanced representative)**.** *For every $C \in \mathcal{C}_n$, there is a unique positive diagonal matrix Δ such that $A_C = \Delta C \Delta \in \mathbb{B}_n$. Writing $D = \mathrm{Diag}(C^{-1})$, the scale and representative are*

$$\Delta = D^{1/4}, \qquad A_C = D^{1/4} C D^{1/4}, \tag{2}$$

and

$$\mathrm{Diag}(A_C) = \mathrm{Diag}(A_C^{-1}) = D^{1/2}. \tag{3}$$

Moreover, for every signed permutation $Q \in \mathfrak{S}_n^{\pm}$,

$$A_{QCQ'} = Q A_C Q', \qquad A_{\mathcal{I}(C)} = A_C^{-1}. \tag{4}$$

The identity $A_{\mathcal{I}(C)} = A_C^{-1}$ shows that normalized correlation inversion corresponds to inversion of the balanced representative. The componentwise scaling is the correlation-matrix specialization of the construction in Lemma 2.4 of Fiedler (1964), which rescales a positive-definite matrix so that its diagonal equals that of its inverse. The proof of Theorem 1, including the scaling formula and its behavior under inversion, is given in Section S2.1.

2.3 Direct hollowness determines the spectral transformation

With the balanced representative fixed, it remains to choose the spectral transformation. Let $g : (0, \infty) \to \mathbb{R}$ be a scalar function. For an eigendecomposition $A = Q\,\mathrm{diag}(a_1, \ldots, a_n)Q'$, define its primary spectral matrix function by $g(A) = Q\,\mathrm{diag}\{g(a_1), \ldots, g(a_n)\}Q'$. Such a transformation treats all eigendirections symmetrically and, when g is a scalar diffeomorphism, can be inverted by applying g^{-1} to the eigenvalues.

We require the complete matrix $g(A_C)$ to be hollow for every C, so inversion does not require completing a missing diagonal. We call this property *direct hollowness*. The normalization $g'(1) = 1$ sets the local scale at independence. For $n \geq 3$, these two requirements uniquely determine g.

Theorem 2 (Rigidity of balanced spectral transformations)**.** *Fix $n \geq 3$. Suppose that $g : (0, \infty) \to \mathbb{R}$ is differentiable at 1 and that*

$$\operatorname{Diag}\{g(A)\} = 0 \qquad \text{for every } A \in \mathbb{B}_n. \tag{5}$$

Then

$$g(a) = \frac{g'(1)}{2}\left(a - a^{-1}\right), \qquad a > 0.$$

Consequently, under the unit local normalization $g'(1) = 1$,

$$g(A) = \frac{1}{2}(A - A^{-1}), \qquad g(a) = \frac{1}{2}(a - a^{-1}) = \sinh(\log a).$$

Differentiability at 1 is the only regularity assumption. When $g'(1) \neq 0$, analyticity, global bijectivity, and the inversion identity $g(a^{-1}) = -g(a)$ follow from the characterization. The proof in Section S2.1 reduces direct hollowness to a scalar functional equation. The restriction $n \geq 3$ is essential: in dimension two, direct hollowness only requires $g(a^{-1}) = -g(a)$, leaving infinitely many normalized choices, including $g(a) = \log a$.

The characterization concerns primary spectral transformations of balanced representatives. Entrywise odd analytic reparametrizations can preserve the properties in Table 1 without belonging to this class; Remark S1 gives an explicit family.

Up to the factor $\frac{1}{2}$, $g(A) = \frac{1}{2}(A - A^{-1})$ is the covariance transformation $\Sigma \mapsto \Sigma - \Sigma^{-1}$ that Zwiernik (2025) studies as an algebraic alternative to the matrix logarithm. The unscaled map $C - C^{-1}$ has diagonal entries $1 - (C^{-1})_{ii} \leq 0$, which are constrained by the correlations. Applying g to the balanced representative A_C yields a hollow matrix.

2.4 The transformation and its inverse

Balance selects A_C, and the rigidity theorem determines $g(a) = (a - a^{-1})/2$. Its scalar inverse, $g^{-1}(b) = b + \sqrt{1 + b^2}$, gives the inverse matrix transformation directly.

Theorem 3 (Balanced correlation parametrization)**.** *For $C \in \mathcal{C}_n$, let A_C be its balanced representative in (2). The* balanced correlation parametrization *is the global real-analytic diffeomorphism $C \mapsto B(C)$ from $\mathcal{C}_n$ onto $\mathbb{H}_n$, with inverse $B \mapsto C(B)$, given by*

$$\begin{aligned} B(C) &= \tfrac{1}{2}(A_C - A_C^{-1}) = \sinh(\log A_C), \\ C(B) &= \operatorname{Cor}(B + \sqrt{I_n + B^2}) = \operatorname{Cor}(e^{\operatorname{arsinh} B}), \qquad B \in \mathbb{H}_n. \end{aligned} \tag{6}$$

Here sinh *and* arsinh *denote the corresponding matrix functions defined by spectral calculus. The matrix $B + \sqrt{I_n + B^2}$ is the unique balanced SPD matrix A satisfying $\frac{1}{2}(A - A^{-1}) = B$.*

Thus the balanced-to-hollow map is itself a real-analytic bijection.

Correlation normalization removes the scale used to construct A_C, so both directions are explicit and require no iterative diagonal correction. For vector coordinates, vecl stacks the strict lower-triangular entries, giving $\beta(C) = \mathrm{vecl}\{B(C)\} \in \mathbb{R}^d$. The reconstruction identities and proof appear in Section S2.2 of the supplement.

Remark 1 (Computation). The forward map uses an SPD solve, diagonal extraction, and matrix products. The inverse uses one symmetric eigendecomposition and a diagonal normalization. Neither map requires an iterative scaling or diagonal-completion step. For numerical stability, if $B = Q\,\mathrm{diag}(\lambda_i)Q'$, evaluate $B + \sqrt{I_n + B^2} = Q\,\mathrm{diag}\big(e^{\mathrm{arsinh}\,\lambda_i}\big)\,Q'$, which avoids cancellation for large negative eigenvalues.

3 Structural properties

The balanced construction preserves the natural symmetries of correlation matrices and gives an exact relation between correlation and precision. We first establish equivariance and inverse consistency, then interpret individual coordinates and study block structure, separability, and behavior near the singular boundary. Proofs appear in Section S2 of the supplement.

3.1 Signed-permutation equivariance

Theorem 4 (Signed-permutation equivariance)**.** *For every $Q \in \mathfrak{S}_n^{\pm}$, every $C \in \mathcal{C}_n$, and every $B \in \mathbb{H}_n$, we have*

$$B(QCQ') = QB(C)Q', \qquad C(QBQ') = QC(B)Q'. \tag{7}$$

Reordering variables or changing their signs applies the same permutation or sign changes to the transformed entries. The definition therefore respects the labeling and sign conventions of the original variables.

3.2 Exact inverse consistency

Theorem 5 (Correlation inversion becomes sign reversal)**.** *For every $C \in \mathcal{C}_n$ and every $B \in \mathbb{H}_n$, we have*

$$B(\mathcal{I}(C)) = -B(C), \qquad C(-B) = \mathcal{I}(C(B)). \tag{8}$$

This distinguishes BCP from GFT, which is not inverse-consistent when $n \geq 3$ (Thanwerdas, 2024). Inverse consistency is not required for a valid parametrization. It matters when transformed matrices are averaged, interpolated, or regularized. The matrices C and $\mathcal{I}(C)$ describe the same dependence system through correlation and normalized precision. BCP places them at opposite points, B and $-B$, in the same Euclidean space. Penalties symmetric about zero therefore treat the two descriptions alike, while averaging and interpolation commute with sign reversal. In particular, along the straight line in coordinates from $B(C)$ to $B(\mathcal{I}(C)) = -B(C)$, the midpoint is $B = 0$, which corresponds to $C = I_n$.

3.3 Marginal and partial correlations

Each BCP entry has a direct interpretation in terms of marginal and full partial correlations.

Proposition 1 (Marginal–partial representation)**.** *Let $C \in \mathcal{C}_n$ and $K = C^{-1}$. Write $\pi_{ij} = -K_{ij}/\sqrt{K_{ii}K_{jj}}$ for the full partial correlation and $\tau_i = K_{ii}^{-1/2}$ for the residual standard deviation of variable i after linear projection on the remaining variables. Then*

$$[B(C)]_{ij} = \frac{C_{ij} + \pi_{ij}}{2\sqrt{\tau_i \tau_j}}, \quad i \neq j. \tag{9}$$

The sign of $[B(C)]_{ij}$ is the sign of $C_{ij} + \pi_{ij}$. Holding the residual standard deviations fixed, its magnitude increases with the absolute value of this sum; holding the sum fixed, it increases as the residual standard deviations decrease. Thus each BCP coordinate is a residual-risk-adjusted average of marginal and partial correlations, rather than an entrywise transformation of the marginal correlation alone.

3.4 Preservation of blocks and symmetries

Proposition 2 (Direct sums and fixed-point classes)**.** *Let $\oplus$ denote the block direct sum. BCP and its inverse preserve direct sums: $B(C_1 \oplus C_2) = B(C_1) \oplus B(C_2)$, and $C(B_1 \oplus B_2) = C(B_1) \oplus C(B_2)$. More generally, for any subgroup $\mathfrak{G} \subseteq \mathfrak{S}_n^{\pm}$,*

$$QCQ' = C \ \forall Q \in \mathfrak{G} \quad \Leftrightarrow \quad QB(C)Q' = B(C) \ \forall Q \in \mathfrak{G}.$$

Thus equicorrelation and other exchangeable or block-symmetric classes map to linear fixed-point subspaces of $\mathbb{H}_n$. Permutation-generated symmetry restrictions also arise in graphical Gaussian models (Højsgaard & Lauritzen, 2008). Section 5 gives the corresponding block formulas and a reduced $G \times G$ implementation based on the canonical representation of Archakov & Hansen (2024).

3.5 Separable correlation matrices

Kronecker products are widely used for separable panel, spatial, and spatio-temporal dependence. BCP preserves their low Kronecker complexity.

Proposition 3 (Kronecker-product identity)**.** *Let $C_k \in \mathcal{C}_{n_k}$, $S_k = B(C_k)$, and $H_k = \sqrt{I_{n_k} + S_k^2}$ for $k = 1, 2$. The balanced representative and BCP satisfy*

$$A_{C_1 \otimes C_2} = A_{C_1} \otimes A_{C_2}, \qquad B(C_1 \otimes C_2) = S_1 \otimes H_2 + H_1 \otimes S_2. \tag{10}$$

Thus a separable correlation matrix maps to a sum of two Kronecker products.

3.6 Boundary behavior

The next result quantifies how approaching the singular boundary affects the size of the BCP coordinates.

Proposition 4 (Properness and a two-sided bound)**.** *The map $C \mapsto B(C)$ from $\mathcal{C}_n$ to $\mathbb{H}_n$ is proper. Quantitatively, write $\ell = \lambda_{\min}(C)$ and $B = B(C)$. Then*

$$\frac{1}{2}\left(\ell^{-1/2} - \ell^{1/2}\right) \le \|B\|_2 \le \frac{1}{2}\left(\frac{n}{\ell} - \frac{\ell}{n}\right), \tag{11}$$

and the left inequality is equivalent to

$$\lambda_{\min}(C) \ge e^{-2\,\mathrm{arsinh}\|B\|_2}. \tag{12}$$

In particular,

$$\lambda_{\min}(C_k) \to 0 \quad \Rightarrow \quad \|B(C_k)\|_F \to \infty. \tag{13}$$

Conversely, a uniform bound on the BCP norm keeps the reconstructed correlation matrices in a compact subset of the open elliptope and hence uniformly away from singularity.

The left inequality in (11) is sharp up to a factor $\sqrt{2}$, attained in the limit $n = 2$, $\rho \to 1$. The bound relates the size of the transformed matrix directly to the conditioning of the correlation matrix it generates.

4 Differentiation and inference

Both directions of the transformation can be differentiated without solving an implicit diagonal-completion problem. Likelihood optimization, filtering, and score-driven updates

usually require the action of a derivative on a direction. The formulas below evaluate that action directly, avoiding the full $d \times d$ Jacobian, where $d = n(n-1)/2$. The corresponding adjoint and likelihood-score formulas are given in Section S3 of the supplement. We first give the forward and inverse derivatives and a closed-form Jacobian determinant, then derive delta-method inference and compare BCP with GFT near independence.

4.1 Closed-form differential operations

Proposition 5 (Forward derivative)**.** *Let $C \in \mathcal{C}_n$, $X \in \mathbb{H}_n$, and define $K = C^{-1}$, $D = \mathrm{Diag}(K)$, $\Delta = D^{1/4}$ and $A = \Delta C \Delta$. Using $\oslash$ for componentwise division, set*

$$\begin{aligned} U_X &= -\frac{1}{4}\,\mathrm{diag}\{\mathrm{diag}(KXK) \oslash \mathrm{diag}(K)\}, \\ Z_X &= \Delta(X + U_X C + C U_X)\Delta. \end{aligned} \tag{14}$$

Then the Jacobian–vector product is

$$\mathrm{d}_C B[X] = \frac{1}{2}\left(Z_X + A^{-1} Z_X A^{-1}\right). \tag{15}$$

In particular,

$$\mathrm{d}_{I_n} B[X] = X. \tag{16}$$

The calculation reuses the solve needed for the transformation and otherwise requires only diagonal extraction, scaling, and matrix products.

Proposition 6 (Inverse derivative)**.** *Let $B = Q\,\mathrm{diag}(\lambda_1, \ldots, \lambda_n) Q'$ and define*

$$a_i = e^{\mathrm{arsinh}(\lambda_i)}, \qquad \Omega_{ij} = \frac{2 a_i a_j}{1 + a_i a_j}. \tag{17}$$

Write $A = Q\,\mathrm{diag}(a_i) Q'$, $e = \mathrm{diag}(A)$, $R = \mathrm{diag}(e^{-1/2})$ and $C = RAR$. For $Y \in \mathbb{H}_n$, let

$$Z_Y = Q\{\Omega \circ (Q'YQ)\}Q', \qquad v_Y = \mathrm{diag}(Z_Y) \oslash e, \qquad V_Y = \mathrm{diag}(v_Y). \tag{18}$$

Here $\circ$ denotes entrywise multiplication. Then

$$\mathrm{d}_B C[Y] = R\left\{Z_Y - \frac{1}{2}(V_Y A + A V_Y)\right\} R. \tag{19}$$

Moreover, $0 < \Omega_{ij} < 2$ for all i, j.

The coefficients in (17) are bounded and require no special branch for repeated eigenvalues. The same eigendecomposition evaluates both the inverse map and its derivative.

Proposition 7 (Jacobian determinant)**.** *For $B \in \mathbb{H}_n$, retain e_i and Ω_{ij} from Proposition 6. With* vecl *denoting strict lower-triangle vectorization, the inverse Jacobian determinant is*

$$j_n(B) := \left|\det \frac{\partial \operatorname{vecl}\{C(B)\}}{\partial \operatorname{vecl}(B)'}\right| = \prod_{i=1}^{n} e_i^{-(n-1)/2} \prod_{1\le i\le j\le n} \Omega_{ij}. \tag{20}$$

For the forward Jacobian $J_C = \partial \operatorname{vecl}\{B(C)\}/\partial \operatorname{vecl}(C)'$, $|\det J_C| = j_n\{B(C)\}^{-1}$.

Once the inverse map has been evaluated, the determinant requires only $O(n^2)$ additional operations, with no full $d \times d$ Jacobian. For numerical evaluation, its logarithm is computed by summing the logs of the positive factors. The formula gives $j_n(0) = 1$ and, for $n = 2$ with $B_{12} = b$, $j_2(B) = (1 + b^2)^{-3/2}$. It is useful for change-of-variables densities; reparametrizing a likelihood as $\ell\{C(B)\}$ does not require a Jacobian-determinant term.

4.2 Delta-method inference

Let J_C be the forward Jacobian defined in Proposition 7. Applying the standard delta method to the analytic map $C \mapsto B(C)$ transfers asymptotic results for a sample correlation matrix directly to the transformed parameters, as follows.

Corollary 1 (Delta method)**.** *For fixed n, if $\hat{C}_T \in \mathcal{C}_n$ satisfies $\sqrt{T}\{\operatorname{vecl}(\hat{C}_T) - \operatorname{vecl}(C)\} \xrightarrow{d} N(0, V_C)$, then*

$$\sqrt{T}\left[\operatorname{vecl}\{B(\hat{C}_T)\} - \operatorname{vecl}\{B(C)\}\right] \xrightarrow{d} N(0, J_C V_C J_C'). \tag{21}$$

At independence, $J_{I_n} = I_d$.

4.3 Relation to the generalized Fisher transformation

The GFT of Archakov & Hansen (2021) uses $\operatorname{Off}(\log C)$ as unrestricted coordinates for the same correlation matrices. Its inverse recovers an omitted diagonal, whereas BCP uses the explicit balanced representative. Despite this difference, the maps agree through second order around independence.

Theorem 6. *Fix n and let $\|\cdot\|$ be a submultiplicative matrix norm. For $C = I_n + E \in \mathcal{C}_n$, with $E \in \mathbb{H}_n$ and $\|E\|$ sufficiently small,*

$$B(C) - \operatorname{Off}(\log C) = \frac{1}{6}\operatorname{Off}(E^3) + \mathcal{O}(\|E\|^4). \tag{22}$$

Both transformations equal $E - \frac{1}{2}\operatorname{Off}(E^2) + \mathcal{O}(\|E\|^3)$. *The remainder constants may depend on the fixed dimension* n.

The proof and the separate expansions appear in Section S4.2. The common linear term gives the same Jacobian, I_d, at independence and hence the same first-order delta-method covariance. More precisely, if $\hat{C}_T - I_n = \mathcal{O}_p(T^{-1/2})$, then $B(\hat{C}_T) - \operatorname{Off}(\log \hat{C}_T) = \mathcal{O}_p(T^{-3/2})$ on the event that $\hat{C}_T$ is positive definite, whose probability tends to one. Near independence, the Jacobians differ at quadratic order in $\|C - I_n\|$.

This local agreement does not extend to equality of the transformations: BCP retains explicit inversion and inverse consistency globally. Supplementary Section S4 gives the exact transition map and its simplification when the diagonal scale commutes with the correlation matrix. The local comparison above is controlled by a matrix norm at fixed dimension; small individual correlations in a large matrix need not make that norm small. The high-dimensional sparsity results in Section 7 therefore require separate structural conditions.

5 Block correlation matrices

Block structures arise naturally with sectors, clusters, and exchangeable groups. BCP preserves a fixed block partition in both directions, allowing the dense matrix operations to use a matrix whose dimension is the number of blocks. Exact preservation holds for all block sizes, including singletons. For clarity, the reduced forward and inverse formulas below are stated for blocks with at least two members; Supplementary Section S5 gives the corresponding singleton formulas.

5.1 A three-block illustration

We begin with a simple example. Consider seven variables divided into three groups of sizes two, two, and three, with common correlations within each group and between each pair of groups. The correlation matrix and its BCP coordinates are

$$\underbrace{\begin{bmatrix} 1.0 & 0.8 & 0.4 & 0.4 & 0.2 & 0.2 & 0.2 \\ 0.8 & 1.0 & 0.4 & 0.4 & 0.2 & 0.2 & 0.2 \\ 0.4 & 0.4 & 1.0 & 0.6 & 0.1 & 0.1 & 0.1 \\ 0.4 & 0.4 & 0.6 & 1.0 & 0.1 & 0.1 & 0.1 \\ 0.2 & 0.2 & 0.1 & 0.1 & 1.0 & 0.3 & 0.3 \\ 0.2 & 0.2 & 0.1 & 0.1 & 0.3 & 1.0 & 0.3 \\ 0.2 & 0.2 & 0.1 & 0.1 & 0.3 & 0.3 & 1.0 \end{bmatrix}}_{= C} \iff \underbrace{\begin{bmatrix} 0 & 1.303 & 0.355 & 0.355 & 0.163 & 0.163 & 0.163 \\ 1.303 & 0 & 0.355 & 0.355 & 0.163 & 0.163 & 0.163 \\ 0.355 & 0.355 & 0 & 0.715 & 0.062 & 0.062 & 0.062 \\ 0.355 & 0.355 & 0.715 & 0 & 0.062 & 0.062 & 0.062 \\ 0.163 & 0.163 & 0.062 & 0.062 & 0 & 0.277 & 0.277 \\ 0.163 & 0.163 & 0.062 & 0.062 & 0.277 & 0 & 0.277 \\ 0.163 & 0.163 & 0.062 & 0.062 & 0.277 & 0.277 & 0 \end{bmatrix}}_{= B(C)}.$$

The gray shading identifies the same blocks in both matrices. The transformation preserves the three-block pattern exactly: entries that are equal under the original partition remain equal after transformation. The remainder of the section establishes this preservation generally and develops reduced formulas that operate directly on the distinct block parameters.

5.2 Correlation and transformed block classes

Fix a partition $\mathcal{P} = (n_1, \ldots, n_G)$ of n, with $n_k \geq 1$ for every k. A block correlation matrix has blocks

$$C_{[k,k]} = (1 - \rho_{kk})I_{n_k} + \rho_{kk}\iota_{n_k}\iota'_{n_k}, \qquad C_{[k,l]} = \rho_{kl}\iota_{n_k}\iota'_{n_l} \quad (k \neq l),$$

subject to $C \succ 0$. Denote this class by $\mathcal{C}_n^{\mathcal{P}}$. The corresponding linear space $\mathbb{H}_n^{\mathcal{P}}$ consists of hollow matrices with

$$B_{[k,k]} = \eta_{kk}(\iota_{n_k}\iota'_{n_k} - I_{n_k}), \qquad B_{[k,l]} = \eta_{kl}\iota_{n_k}\iota'_{n_l} \quad (k \neq l). \tag{23}$$

For a singleton block, these expressions reduce to $C_{[k,k]} = [1]$ and $B_{[k,k]} = [0]$, with no within-block parameter. Both classes have $G(G-1)/2 + |\{k : n_k > 1\}|$ free parameters: one for each unordered pair of blocks and one within each nonsingleton block.

5.3 Exact preservation

Theorem 7 (Exact preservation of block symmetry)**.** *For every fixed partition with $n_k \geq 1$, the transformation and its inverse restrict to mutually inverse real-analytic diffeomorphisms*

$$\mathcal{C}_n^{\mathcal{P}} \underset{C(\cdot)}{\overset{B(\cdot)}{\rightleftarrows}} \mathbb{H}_n^{\mathcal{P}}.$$

Thus the partition and its constant-entry pattern are preserved in both directions.

This preservation follows directly from equivariance. The two block classes are the fixed-point sets of independent permutations within each block, and a bijective map that commutes with these permutations must map one fixed-point set onto the other. The same argument applies to fixed-point classes of other subgroups of signed permutations.

For fixed block sizes $n_k \geq 2$, Theorem 7 provides a new parametrization of block correlation matrices by an unrestricted symmetric $G \times G$ matrix (η_{kl}). Its diagonal entries specify within-block coordinates, while its off-diagonal entries specify between-block coordinates. Every choice yields a unique positive-definite correlation matrix with the prescribed block structure.

This provides an alternative to the GFT-based block parametrization discussed by Tong & Hansen (2023), with both the forward and inverse maps available in closed form. For singleton blocks, the corresponding within-block coordinates are omitted.

5.4 Reduced forward transformation

For the reduced formulas in this subsection, assume $n_k \geq 2$ for every k. Define the $G \times G$ core $R = (r_{kl})$ and the within-block contrast eigenvalues λ_k by $r_{kk} = 1+(n_k-1)\rho_{kk}$, $r_{kl} = \rho_{kl}\sqrt{n_k n_l}$ for $k \neq l$, and $\lambda_k = 1 - \rho_{kk}$. Positive definiteness of C is equivalent to $R \succ 0$ and $\lambda_k > 0$ for every k.

Theorem 8 (Reduced forward transformation)**.** *For $C \in \mathcal{C}_n^{\mathcal{P}}$, define $\delta_k > 0$ and Δ by*

$$\delta_k^4 = \frac{(R^{-1})_{kk}}{n_k} + \frac{n_k - 1}{n_k \lambda_k}, \qquad \Delta = \operatorname{diag}(\delta_1, \ldots, \delta_G). \tag{24}$$

Then $\operatorname{Diag}(C^{-1})$ *is constant within block k, with value δ_k^4. Set*

$$M = \frac{1}{2}\left(\Delta R \Delta - \Delta^{-1} R^{-1} \Delta^{-1}\right), \qquad \zeta_k = \frac{1}{2}\left(\delta_k^2 \lambda_k - \delta_k^{-2} \lambda_k^{-1}\right). \tag{25}$$

The entries of $B(C)$ in (23) are

$$\eta_{kl} = \frac{M_{kl}}{\sqrt{n_k n_l}} \quad (k \neq l), \qquad \eta_{kk} = -\zeta_k = \frac{M_{kk}}{n_k - 1}. \tag{26}$$

Thus the forward transformation requires one $G \times G$ inverse and scalar operations. The block means interact through R, while each block contributes one scalar contrast.

5.5 Reduced inverse transformation

Again assume $n_k \geq 2$ for every k. Given $B \in \mathbb{H}_n^{\mathcal{P}}$, form the reduced core

$$H_{kk} = (n_k - 1)\eta_{kk}, \qquad H_{kl} = \eta_{kl}\sqrt{n_k n_l} \ (k \neq l), \qquad \zeta_k = -\eta_{kk}. \tag{27}$$

Theorem 9 (Reduced inverse transformation)**.** *Let $f(x) = x + \sqrt{1 + x^2} = e^{\operatorname{arsinh} x}$ and define $F = f(H) = H + \sqrt{I_G + H^2}$ and $a_k = f(\zeta_k)$. Set*

$$e_k = \frac{F_{kk} + (n_k - 1)a_k}{n_k}. \tag{28}$$

Then $C = C(B)$ has block correlations

$$\rho_{kk} = \frac{F_{kk} - a_k}{n_k e_k}, \qquad \rho_{kl} = \frac{F_{kl}}{\sqrt{n_k n_l e_k e_l}}, \quad k \neq l. \tag{29}$$

Corollary 2 (Reduced computational dimension)**.** *If only the distinct block parameters are required, the forward map uses one $G \times G$ inverse and the inverse map uses one $G \times G$ principal square root, followed by scalar operations. Their dense matrix-function cost is $O(G^3)$ rather than $O(n^3)$. Constructing the full matrix still requires $O(n^2)$ output work.*

5.6 Equicorrelation matrices

The one-block case, $G = 1$, corresponds to an equicorrelation matrix. It yields explicit scalar formulas for BCP and its inverse and provides a simple comparison with GFT.

Proposition 8 (BCP for equicorrelation matrices)**.** *Let $n \geq 2$ and $C_n(\rho) = (1-\rho)I_n + \rho\iota\iota'$, with $-1/(n-1) < \rho < 1$. Then $B(C_n(\rho)) = b_n(\rho)(\iota\iota' - I_n)$, where*

$$b_n(\rho) = \frac{\rho\{2 + (n-2)\rho\}}{2\sqrt{\{1 + (n-2)\rho\}(1-\rho)\{1 + (n-1)\rho\}}}. \tag{30}$$

The inverse is also explicit. Given $b \in \mathbb{R}$, set $a_1 = (n-1)b + \sqrt{1 + (n-1)^2 b^2}$ and $a_2 = -b + \sqrt{1 + b^2}$. Then

$$\rho = \frac{a_1 - a_2}{a_1 + (n-1)a_2}. \tag{31}$$

Let $z(\rho) = \operatorname{atanh}(\rho)$ denote Fisher's z-transformation. The bivariate BCP takes the form

$$B\left(\begin{bmatrix} 1 & \rho \\ \rho & 1 \end{bmatrix}\right) = \sinh\left(\begin{bmatrix} 0 & z(\rho) \\ z(\rho) & 0 \end{bmatrix}\right) = \begin{bmatrix} 0 & \frac{\rho}{\sqrt{1-\rho^2}} \\ \frac{\rho}{\sqrt{1-\rho^2}} & 0 \end{bmatrix}.$$

Thus, the BCP coordinate is the hyperbolic sine of Fisher's z-transformation, whereas the GFT coordinate equals Fisher's z itself.

For general n, the common GFT coordinate of an equicorrelation matrix is $g_n(\rho) = n^{-1}\log\{[1 + (n-1)\rho]/(1-\rho)\}$. The exact relation between the two coordinates is

$$g_n(\rho) = \frac{1}{n}\left[\operatorname{arsinh}\big((n-1)b_n(\rho)\big) + \operatorname{arsinh}\big(b_n(\rho)\big)\right]. \tag{32}$$

For fixed n, these coordinates agree through second order as $\rho \to 0$, in accordance with the general local comparison in Section 4.3. A proof of Proposition 8 and identity (32) is given

in Supplementary Section S2.6. The identity is a scalar instance of the general commuting relation in Supplementary Proposition S1.

6 BCP for selected structured correlation matrices

BCP is explicit for every positive-definite correlation matrix, but its forward formula becomes particularly transparent when the precision matrix is known analytically. Let $K = C^{-1}$ and $\delta_i = K_{ii}^{1/4}$. Directly from the definition, $[B(C)]_{ij} = \frac{1}{2}(\delta_i\delta_j C_{ij} - \frac{1}{\delta_i\delta_j}K_{ij})$, $i \neq j$. Thus a structured precision matrix immediately gives a simplified BCP expression, without a matrix eigendecomposition in the forward direction. We consider arrowhead, Gaussian-tree, moving-average, autoregressive, and standard factor correlations. The time-series examples distinguish banded correlations from banded precision matrices.

6.1 Arrowhead correlation matrices

For $\rho \in \mathbb{R}^r$ with $\rho'\rho < 1$, consider the $(r+1) \times (r+1)$ arrowhead correlation matrix

$$C^\star(\rho) = \begin{pmatrix} 1 & \rho' \\ \rho & I_r \end{pmatrix}. \tag{33}$$

This is a unit-diagonal instance of the symmetric arrowhead matrices studied by O'Leary & Stewart (1990). It is also the auxiliary correlation matrix for $(Z, U')'$ used by Tong & Hansen (2026), who derive a tractable expression under GFT.

Proposition 9 (BCP coordinates of an arrowhead correlation matrix)**.** *Let* $\omega = \sqrt{1-\rho'\rho}$ *and* $h_j = \omega^2 + \rho_j^2$ *for* $j = 1, \ldots, r$*, and define* $R_\rho = \operatorname{diag}\left(h_1^{1/4}, \ldots, h_r^{1/4}\right)$ *and* $v_\rho = R_\rho^{-1}\rho$*. Then*

$$B\left(C^\star(\rho)\right) = \begin{pmatrix} 0 & \eta_\rho' \\ \eta_\rho & \Psi_\rho \end{pmatrix}, \tag{34}$$

where

$$\eta_\rho = \frac{1}{2\omega}\left(R_\rho + R_\rho^{-1}\right)\rho, \qquad \Psi_\rho = -\frac{1}{2\omega}\operatorname{Off}\left(v_\rho v_\rho'\right).$$

Equivalently, for $j \neq k$*,*

$$[\eta_\rho]_j = \frac{\rho_j}{2\omega}\left(h_j^{1/4} + h_j^{-1/4}\right), \qquad [\Psi_\rho]_{jk} = -\frac{\rho_j\rho_k}{2\omega(h_jh_k)^{1/4}}, \qquad [\Psi_\rho]_{jj} = 0. \tag{35}$$

The vector η_ρ preserves the zero pattern and signs of ρ. The block Ψ_ρ records linear partial associations among the peripheral variables, although their block in $C^\star(\rho)$ is the identity.

This illustrates why a zero marginal correlation need not produce a zero BCP coordinate at finite dimension.

6.2 Gaussian-tree correlation matrices

Let (V, E) be a tree and associate an edge correlation $\theta_{ij} \in (-1, 1)$ with every $\{i, j\} \in E$. The corresponding standardized Gaussian tree has

$$C_{ij} = \prod_{e \in \mathrm{path}(i,j)} \theta_e, \qquad C_{ii} = 1. \tag{36}$$

Its precision matrix $K = C^{-1}$ is supported on the tree:

$$K_{ij} = \begin{cases} -\dfrac{\theta_{ij}}{1-\theta_{ij}^2}, & \{i,j\} \in E, \\ 0, & \{i,j\} \notin E, \end{cases} \quad i \neq j, \quad \text{and} \quad K_{ii} = 1 + \sum_{j:\{i,j\}\in E} \frac{\theta_{ij}^2}{1-\theta_{ij}^2}. \tag{37}$$

Proposition 10 (BCP coordinates of a Gaussian-tree correlation matrix)**.** *Let* $\delta_i = K_{ii}^{1/4}$. *For* $i \neq j$,

$$[B(C)]_{ij} = \begin{cases} \dfrac{1}{2}\left\{\delta_i\delta_j\theta_{ij} + \dfrac{\theta_{ij}}{(1-\theta_{ij}^2)\delta_i\delta_j}\right\}, & \{i,j\} \in E, \\ \dfrac{1}{2}\delta_i\delta_j \displaystyle\prod_{e \in \mathrm{path}(i,j)} \theta_e, & \{i,j\} \notin E. \end{cases} \tag{38}$$

The homogeneous path tree gives the AR(1) correlation matrix $C_{ij} = \rho^{|i-j|}$, which is a special case of the autoregressive family considered in Section 6.4.

6.3 Moving-average correlation matrices

Consider the MA(q) process $x_t = \sum_{\ell=0}^{q} \theta_\ell \varepsilon_{t-\ell}$, where $\theta_0 = 1$ and ε_t is zero-mean, unit-variance white noise. For $n > q \geq 1$, the correlation matrix of $(x_1, \ldots, x_n)'$ is banded Toeplitz, with $C_{ij} = \rho_{|i-j|}$ and

$$s = \sum_{\ell=0}^{q} \theta_\ell^2, \qquad \rho_h = \begin{cases} s^{-1} \displaystyle\sum_{\ell=0}^{q-h} \theta_\ell\theta_{\ell+h}, & 0 \leq h \leq q, \\ 0, & h > q. \end{cases} \tag{39}$$

This is the usual finite-order moving-average covariance structure (Hamilton, 1994, Chapter 3). Its inverse can be obtained from a finite filter recursion and a correction for the q presample

innovations. Define

$$\psi_0 = 1, \qquad \psi_k = -\sum_{\ell=1}^{\min(q,k)} \theta_\ell \psi_{k-\ell}, \quad k = 1, \dots, n-1, \tag{40}$$

and set $\psi_k = 0$ for $k < 0$ and $\theta_k = 0$ for $k > q$. Let $F \in \mathbb{R}^{n\times n}$ and $H \in \mathbb{R}^{n\times q}$ have entries $F_{ij} = \psi_{i-j}$ and $H_{ia} = \theta_{i+a-1}$, and put $W = F'F$ and $M = I_q + H'WH$.

Proposition 11 (BCP coordinates of a moving-average correlation matrix)**.** *The matrix in* (39) *is positive definite, and its precision matrix and balancing weights satisfy*

$$K = s\left(W - WHM^{-1}H'W\right), \qquad \delta_i = K_{ii}^{1/4}. \tag{41}$$

For $i \neq j$,

$$[B(C)]_{ij} = \frac{1}{2}\left(\delta_i\delta_j\rho_{|i-j|} - \frac{K_{ij}}{\delta_i\delta_j}\right). \tag{42}$$

In particular, $[B(C)]_{ij} = -K_{ij}/(2\delta_i\delta_j)$ whenever $|i-j| > q$.

The only matrix inverse in (41) has dimension q; the formula does not require invertibility of the MA process. For MA(1), $\rho_1 = \theta_1/(1+\theta_1^2)$ and C is tridiagonal. More generally, although every correlation beyond lag q is zero, the corresponding precision entries are generally nonzero. The BCP matrix is therefore generally dense, despite the finite range of the marginal correlations.

6.4 Autoregressive correlation matrices

Consider a zero-mean, stationary causal AR(p) process with unit marginal variance,

$$x_t = \sum_{\ell=1}^{p} \phi_\ell x_{t-\ell} + \varepsilon_t, \qquad \mathrm{Var}(\varepsilon_t) = \sigma^2 > 0,$$

where ε_t is zero-mean white noise and $1 - \sum_{\ell=1}^{p}\phi_\ell z^\ell$ has all its roots outside the unit circle. For $n > p \geq 1$, its correlation matrix is Toeplitz, $C_{ij} = \rho_{|i-j|}$, where $\rho_0 = 1$, $\rho_h = \sum_{\ell=1}^{p}\phi_\ell\rho_{|h-\ell|}$ for $h \geq 1$, and $\sigma^2 = 1 - \sum_{\ell=1}^{p}\phi_\ell\rho_\ell$. Its precision matrix is banded. Let $C_p = (\rho_{|i-j|})_{i,j=1}^{p}$, let $E_p = (I_p, 0) \in \mathbb{R}^{p\times n}$, and define $r_s = e_s - \sum_{\ell=1}^{p}\phi_\ell e_{s-\ell}$ for $s = p+1, \dots, n$, where e_s is the sth coordinate vector in $\mathbb{R}^n$.

Proposition 12 (BCP coordinates of an autoregressive correlation matrix)**.** *The precision matrix is*

$$K = E_p' C_p^{-1} E_p + \frac{1}{\sigma^2}\sum_{s=p+1}^{n} r_s r_s', \qquad K_{ij} = 0 \quad \text{if } |i-j| > p. \tag{43}$$

With $\delta_i = K_{ii}^{1/4}$ and $h = |i-j|$, the off-diagonal BCP entries are

$$[B(C)]_{ij} = \begin{cases} \frac{1}{2}\left(\delta_i\delta_j\rho_h - \frac{K_{ij}}{\delta_i\delta_j}\right), & 1 \le h \le p, \\ \frac{1}{2}\delta_i\delta_j\rho_h, & h > p. \end{cases} \tag{44}$$

Equation (43) includes the finite-sample boundary corrections and requires only a $p \times p$ inverse. Beyond lag p, each BCP coordinate is a positive rescaling of the corresponding correlation, so its sign and zero status are preserved exactly. For fixed p, only $O(np)$ pairs receive a precision correction. Scalar formulas for the interior entries are given in (S.3) of the supplement.

When $p = 1$ and $\phi_1 = \rho$, C coincides with the correlation matrix of the homogeneous Gaussian path in Section 6.2. In this case, $K_{11} = K_{nn} = 1/(1-\rho^2)$ and $K_{ii} = (1+\rho^2)/(1-\rho^2)$ for $2 \le i \le n-1$. With $\delta_i = K_{ii}^{1/4}$,

$$[B(C)]_{ij} = \frac{1}{2}\delta_i\delta_j\rho^{|i-j|} + \frac{\rho\,\mathbb{1}\{|i-j|=1\}}{2(1-\rho^2)\delta_i\delta_j}, \qquad i \ne j. \tag{45}$$

The endpoint and interior diagonal values differ, so the transformed matrix need not be Toeplitz. Gaussianity is not needed for the correlation or BCP formulas above.

6.5 Standard factor-model correlation matrices

Consider standardized variables with r orthogonal common factors. Let the ith row of the $n \times r$ loading matrix Λ be λ_i' and set

$$C = Q + \Lambda\Lambda', \qquad Q = \mathrm{diag}(q_1, \ldots, q_n), \qquad q_i = 1 - \lambda_i'\lambda_i > 0. \tag{46}$$

Then C is a correlation matrix. Define M and $\delta_i > 0$ by

$$M = I_r + \Lambda' Q^{-1}\Lambda, \qquad \delta_i^4 = \frac{1}{q_i} - \frac{\lambda_i' M^{-1}\lambda_i}{q_i^2}. \tag{47}$$

Proposition 13 (BCP coordinates of a factor-model correlation matrix)**.** *For the matrix in (46) and $i \ne j$,*

$$[B(C)]_{ij} = \frac{1}{2}\left\{\delta_i\delta_j\lambda_i'\lambda_j + \frac{\lambda_i' M^{-1}\lambda_j}{q_i q_j \delta_i\delta_j}\right\}. \tag{48}$$

Equivalently, if

$$u_i = \delta_i\lambda_i, \qquad v_i = \frac{M^{-1/2}\lambda_i}{q_i\delta_i}, \tag{49}$$

where $M^{-1/2}$ is the symmetric positive-definite inverse square root, then

$$[B(C)]_{ij} = \frac{1}{2}\left(u_i' u_j + v_i' v_j\right), \qquad i \neq j. \tag{50}$$

Thus each off-diagonal BCP coordinate averages two loading inner products: one formed from the risk-scaled original loadings and the other from the precision-dual loadings. Evaluation uses $r \times r$ matrix operations and pairwise inner products, avoiding an $n \times n$ eigendecomposition. These finite-dimensional formulas do not require pervasive factors; the additional conditions in Assumption 1 yield the asymptotic sparsity result in Theorem 10.

For a one-factor model, write $\Lambda = \beta$, $q_i = 1 - \beta_i^2$, and $\kappa = 1 + \sum_{l=1}^{n} \beta_l^2/q_l$. Then $\delta_i^4 = q_i^{-1} - \beta_i^2/(\kappa q_i^2)$ and $[B(C)]_{ij} = \frac{\beta_i \beta_j}{2}\left(\delta_i \delta_j + \frac{1}{\kappa q_i q_j \delta_i \delta_j}\right)$ for $i \neq j$.

7 Sparsity preservation in high dimensions

Equicorrelation provides a simple illustration of how transformed coordinates behave as the dimension increases. For a fixed correlation $0 < \rho < 1$, Proposition 8 gives

$$b_n(\rho) \longrightarrow \frac{\rho}{2\sqrt{1-\rho}} > 0, \qquad g_n(\rho) = \frac{1}{n} \log \frac{1 + (n-1)\rho}{1 - \rho} \longrightarrow 0.$$

The off-diagonal LS coordinates also equal $g_n(\rho)$. Thus BCP retains a nonvanishing coordinate for a fixed nonzero correlation, whereas GFT and LS coordinates shrink. This example motivates the question of whether vanishing and nonvanishing correlations remain distinguishable in transformed coordinates.

The factor-model formulas in Proposition 13 provide a basis for addressing this question. Cholesky and spherical parametrizations have also been developed for estimation with a given pattern of zero correlations (Saxena et al., 2023; Huang et al., 2025). Here we study the asymptotic correspondence between marginal correlations and unrestricted BCP coordinates under suitable factor conditions. Each BCP coordinate then approximates a positively rescaled correlation uniformly over all pairs, keeping weak marginal associations small without driving material associations to zero. This correspondence permits support recovery under suitable signal and estimation-error conditions, although setting a BCP coordinate to zero need not produce an exact zero correlation at finite dimension. All proofs and detailed comparisons are collected in Supplementary Section S7.

7.1 Factor strength and residual variation

Assumption 1 (Increasing factor strength with diagonal residual covariance)**.** *For each n, let*

$$C_n = \Lambda_n \Lambda_n' + \Omega_n \in \mathcal{C}_n, \qquad \Omega_n = \operatorname{diag}(\omega_{1,n}, \ldots, \omega_{n,n}).$$

The matrix Λ_n has $r_n \geq 1$ linearly independent columns. For a constant $a > 0$ independent of n,

$$a \leq \omega_{i,n} \leq 1, \qquad \mu_n := \lambda_{\min}(\Lambda_n' \Omega_n^{-1} \Lambda_n) \to \infty. \tag{51}$$

The transpose of row i of Λ_n is denoted by $\lambda_{i,n}$.

Here $\omega_{i,n}$ measures residual variance after removing the common factors; τ_i^2 in Proposition 1 measures residual variance after projection on the remaining observed variables. The diagonal residual covariance requires the residuals to be mutually uncorrelated, while the lower bound on their variances prevents any variable from being almost entirely explained by the factors. Since C_n has unit diagonal, the loadings satisfy $\|\lambda_{i,n}\|^2 = 1 - \omega_{i,n} \leq 1 - a$. To interpret the factor-strength condition, write

$$\mu_n = \min_{\|v\|_2 = 1} v' \Lambda_n' \Omega_n^{-1} \Lambda_n v = \min_{\|v\|_2 = 1} \sum_{i=1}^{n} \frac{(\lambda_{i,n}' v)^2}{\omega_{i,n}}.$$

Here $v \in \mathbb{R}^{r_n}$ selects a unit direction in factor space, corresponding to a linear combination of the factors, and $\lambda_{i,n}' v$ is variable i's loading in that direction. Dividing its squared loading by $\omega_{i,n}$ measures its contribution relative to residual noise, giving greater weight to variables with smaller residual variances. Summing across variables gives the aggregate strength of that direction, and taking the minimum identifies the weakest direction.

Thus, $\mu_n \to \infty$ requires factor strength to diverge uniformly across all unit directions as the panel grows. Increasing dimension alone is insufficient: merely adding variables unrelated to the weakest direction does not strengthen it. The condition does not require each direction to affect a fixed fraction of the panel. The number of factors may also increase, although

$$r_n \mu_n \leq \operatorname{tr}(\Lambda_n' \Omega_n^{-1} \Lambda_n) \leq \frac{n(1-a)}{a}$$

implies $r_n = o(n)$.

A familiar special case is a fixed number of pervasive factors with $\mu_n \geq \kappa n$ for some $\kappa > 0$. The assumption also allows semi-strong factors, for example $\mu_n \asymp n^\alpha$ with $0 < \alpha < 1$ (Chudik et al., 2011). With one factor per disjoint group and all within-group loading magnitudes uniformly bounded away from zero, $\mu_n \asymp \min_k n_k$, where n_k is the size of group k. The

condition therefore holds when the smallest group grows. More general loading patterns must satisfy the same eigenvalue condition. The assumption permits heterogeneous loadings and residual variances and does not require the proportion of nonzero correlations to vanish.

Here sparsity concerns marginal uncorrelatedness, $C_{ij,n} = 0$, rather than zeros of the precision matrix. For Gaussian vectors, covariance zeros encode marginal independence (Chaudhuri et al., 2007), whereas precision zeros encode conditional independence given the remaining variables (Dempster, 1972). Related screening methods for correlation and partial-correlation hubs are studied by Hero & Rajaratnam (2012).

7.2 Entrywise preservation by BCP

Let $K_n = C_n^{-1}$, $\delta_{i,n} = K_{ii,n}^{1/4}$, and $B_n = B(C_n)$. The exact coordinate formula is

$$B_{ij,n} = \frac{1}{2}\left(\delta_{i,n}\delta_{j,n}C_{ij,n} - \frac{K_{ij,n}}{\delta_{i,n}\delta_{j,n}}\right), \qquad i \neq j. \tag{52}$$

The weakest factor strength also controls the approximation error. Under Assumption 1, Woodbury's identity expresses K_n as the diagonal matrix Ω_n^{-1} minus a factor correction involving $(I_{r_n} + \Lambda_n'\Omega_n^{-1}\Lambda_n)^{-1}$. Since

$$\left\|(I_{r_n} + \Lambda_n'\Omega_n^{-1}\Lambda_n)^{-1}\right\|_2 = \frac{1}{1+\mu_n},$$

the bounds on loadings and residual variances imply that the off-diagonal precision entries are uniformly $O(\mu_n^{-1})$, while the diagonal scaling remains bounded. The following theorem translates these bounds into a uniform approximation of BCP coordinates by positively rescaled correlations.

Theorem 10 (Uniform preservation of the correlation entries)**.** *Under Assumption 1, set* $h_n = \{a^2(1+\mu_n)\}^{-1}$ *and* $K_a = \frac{1}{2} + \frac{1}{4}a^{-1/4}$. *Then*

$$B_{ij,n} = s_{ij,n}C_{ij,n} + R_{ij,n}, \qquad s_{ij,n} = \frac{1}{2(\omega_{i,n}\omega_{j,n})^{1/4}}, \tag{53}$$

where, uniformly over $i \neq j$,

$$\frac{1}{2} \leq s_{ij,n} \leq \frac{1}{2\sqrt{a}}, \qquad |R_{ij,n}| \leq K_a h_n = O(\mu_n^{-1}). \tag{54}$$

At an exact zero, the sharper bound is

$$C_{ij,n} = 0 \quad \Rightarrow \quad |B_{ij,n}| \le \frac{h_n}{2}. \tag{55}$$

Because the scaling is positive and bounded above and away from zero, (53) gives, uniformly over $i \neq j$,

$$|B_{ij,n}| \le \frac{|C_{ij,n}|}{2\sqrt{a}} + K_a h_n, \qquad |C_{ij,n}| \le 2|B_{ij,n}| + 2K_a h_n, \tag{56}$$

with $h_n \to 0$. Thus, for a fixed pair, or along any sequence of pairs (i_n, j_n), the coordinate $B_{i_n j_n, n}$ vanishes as $n \to \infty$ if and only if the correlation $C_{i_n j_n, n}$ does. A correlation bounded away from zero retains a nonvanishing coordinate, while a zero or vanishing correlation has a vanishing coordinate. If $\mu_n |C_{i_n j_n, n}| \to \infty$, the relative approximation error vanishes and the signs agree eventually. The uniform entrywise bound also allows statements about all pairs simultaneously; it does not assert a vanishing operator-norm error. This preservation concerns the limit $n \to \infty$. At finite dimension, (52) gives $B_{ij,n} = 0$ at a correlation zero only when $K_{ij,n} = 0$ as well. Increasing dimension alone is insufficient; Supplementary Remark S2 gives a fixed-block example. For pervasive factors, the remainder is $O(n^{-1})$; if $\mu_n \asymp n^{\alpha}$, it is $O(n^{-\alpha})$.

The factor setting provides an interpretable sufficient regime for this equivalence. More generally, it suffices that the precision diagonals are uniformly bounded and the off-diagonal precision entries vanish uniformly: $\max_i K_{ii,n} \le M < \infty$, $\varepsilon_n := \max_{i \neq j} |K_{ij,n}| \to 0$. The first condition means that no standardized variable becomes almost perfectly linearly predictable from all the others: its prediction residual variance is $K_{ii,n}^{-1} \ge M^{-1}$. Under this bound, the second condition is equivalent to uniformly vanishing full partial correlations. Indeed, since $K_{ii,n} \ge 1$, (52) expresses $B_{ij,n}$ as $\frac{1}{2}(K_{ii,n}K_{jj,n})^{1/4} C_{ij,n}$ plus an error bounded by $\varepsilon_n/2$, with the multiplier between $1/2$ and $\sqrt{M}/2$. Thus the same vanishing-coordinate equivalence holds. Assumption 1 implies these conditions with $M = a^{-1}$ and $\varepsilon_n \le h_n = O(\mu_n^{-1})$; we retain that setting for the explicit rates and support results below.

7.3 Support recovery

Thresholding is widely used for sparse covariance estimation (Bickel & Levina, 2008). Related work studies large-scale screening for variables with strong correlations (Hero & Rajaratnam, 2011; Wei et al., 2023). Here a common magnitude threshold on BCP coordinates can distinguish null and nonnull pairs when the smallest nonzero correlation dominates the approximation error.

Corollary 3 (Recovery of the entire support)**.** *Under Assumption 1, let* $\mathcal{S}_n = \{(i,j) : i < j,\ C_{ij,n} \neq 0\}$ *and* $m_n = \min_{(i,j)\in\mathcal{S}_n} |C_{ij,n}|$*. If* $\mu_n^{-1} = o(\tau_n)$ *and* $\tau_n = o(m_n)$*, then, for all sufficiently large* n*,*

$$\{(i,j) : i < j,\ |B_{ij,n}| > \tau_n\} = \mathcal{S}_n.$$

The retained coordinates also have the signs of the corresponding correlations. At any finite n*, it is sufficient to choose*

$$h_n/2 < \tau_n < m_n/2 - K_a h_n,$$

whenever this interval is nonempty. These uniform finite-dimension bounds are sufficient and can be conservative.

The condition concerns the entire support, not just a fixed pair. For example, if all nonzero correlations are bounded away from zero, $\tau_n = \mu_n^{-1/2}$ is admissible. If the support is empty, only the null bound is needed. A separating threshold exists when $\mu_n m_n \to \infty$. For estimated coordinates, support recovery also requires estimation error to be smaller than the threshold.

Corollary 4 (Support recovery from estimated coordinates)**.** *Under Assumption 1, let* m_n *be the smallest nonzero correlation magnitude and let* $B_n = B(C_n)$*. Suppose symmetric hollow estimates satisfy*

$$\max_{i\neq j} |\hat{B}_{ij,n} - c_n B_{ij,n}| = O_p(e_n)$$

for positive scalars c_n*, possibly random, such that* c_n *and* c_n^{-1} *are* $O_p(1)$*. If*

$$\mu_n^{-1} + e_n = o(\tau_n), \qquad \tau_n = o(m_n),$$

then thresholding $\hat{B}_n$ *at* τ_n *recovers* $\mathcal{S}_n$ *and the signs of its correlations with probability tending to one as* $n \to \infty$*.*

The error rate e_n depends on the estimator. The factor c_n allows common multiplicative bias without changing the asymptotic separation orders; a particular finite-sample threshold still depends on scale. For independent Gaussian observations with $n, T \to \infty$ and n/T bounded away from one from below, Supplementary Proposition S2 establishes this condition for $\hat{B}_n = B(\hat{C}_n)$ with $c_n = (1 - n/T)^{-1/2}$ and $e_n = \sqrt{\log n/T}$. The result accommodates a nonvanishing dimension-to-sample-size ratio.

7.4 Reconstruction after imposing zero coordinates

Support recovery concerns the forward coordinates. For modeling, it is also useful to know whether imposing their zeros retains the original correlations after inversion. The

following result gives such a guarantee with a bounded number of factors and allows arbitrary heterogeneous loadings subject to Assumption 1.

Proposition 14 (Reconstruction from the correlation support)**.** *Suppose Assumption 1 holds and* $\sup_n r_n < \infty$*. Let* $\tilde{B}_n$ *equal* $B_n = B(C_n)$ *except that its entries are set to zero wherever* $C_{ij,n} = 0$*. Then*

$$\max_{i,j} \left| [C(\tilde{B}_n)]_{ij} - C_{ij,n} \right| = O(\mu_n^{-1}).$$

In the pervasive case $\mu_n \geq \kappa n$*, this error is* $O(n^{-1})$*.*

In the pervasive case, the trace bound $r_n \mu_n \leq n(1-a)/a$ gives $r_n \leq (1-a)/(a\kappa)$, so the bounded-factor condition is automatic. The result also covers a bounded number of semi-strong factors, with the rate determined by the weakest factor direction.

The proposition concerns zeroing coordinates at population correlation zeros and retaining the remaining coordinates unchanged. It controls the entire reconstructed matrix, including its originally zero entries. Because the zero locations are supplied, no minimum-signal condition is needed; identifying them from data requires separate support-recovery conditions. The reconstructed matrix need not retain the original factor representation. Positive definiteness follows from the inverse map at every dimension.

7.5 Comparison with the GFT, InvC, and LS methods

What separates BCP from GFT, InvC, and LS is the relation between a coordinate and the corresponding marginal correlation. Write $H_n = \mathrm{Off}(\log C_n)$ for GFT; InvC uses the off-diagonal entries of $K_n = C_n^{-1}$. Under Assumption 1,

$$\max_{i \neq j} |H_{ij,n}| = O(\log(1+\mu_n)/\mu_n), \qquad \max_{i \neq j} |K_{ij,n}| \leq h_n = O(\mu_n^{-1}),$$

including at correlations bounded away from zero. The InvC bound follows directly from Woodbury's identity. In the pervasive special case $\mu_n \geq \kappa n$ with homogeneous residual variance $\Omega_n = \omega I_n$, let $Q_n = \Lambda_n' \Lambda_n / n$. The leading terms are

$$H_{ij,n} = \frac{\log n}{n} \lambda_{i,n}' Q_n^{-1} \lambda_{j,n} + O(n^{-1}), \qquad K_{ij,n} = -\frac{1}{\omega n} \lambda_{i,n}' Q_n^{-1} \lambda_{j,n} + O(n^{-2}),$$

whereas $C_{ij,n} = \lambda_{i,n}' \lambda_{j,n}$ for $i \neq j$. Thus both leading terms depend on a different inner product from the correlation itself, and their zeros need not agree with correlation zeros.

For LS, write $S_n = \mathrm{Log}_{\mathrm{LS}}(C_n) = \log(D_n C_n D_n)$, where the positive diagonal matrix D_n satisfies $D_n C_n D_n \iota_n = \iota_n$. If its largest-to-smallest diagonal ratio is uniformly bounded, then $\max_{i \neq j} |S_{ij,n}| = O(\log(1+\mu_n)/\mu_n)$ as well. This extra scaling condition does not follow from

Assumption 1. The equicorrelation example at the beginning of this section illustrates these contrasting limits explicitly.

The fact that all GFT coordinates vanish does not itself preclude support recovery, because coordinates associated with zero correlations could vanish faster than those associated with nonzero correlations. However, the factor conditions do not guarantee this separation. The counterexample in Supplementary Example S1 has a zero correlation whose GFT coordinate has magnitude of order $(\log n)/n$, whereas a fixed nonzero correlation has a coordinate of order n^{-1}. The zero-correlation coordinate therefore vanishes more slowly, preventing a common magnitude threshold from separating the two pairs, even after common rescaling.

The same example establishes failure of threshold separation for InvC, while Supplementary Example S2 establishes it for LS within the factor class. Propositions S3 to S5 give the GFT and LS formulas and their conditions. Thus GFT, InvC, and LS do not share BCP's general coordinate-thresholding guarantee. All four maps remain invertible and preserve block-diagonal zeros; the comparison concerns entrywise marginal support, not loss of information or the exclusion of special subclasses.

8 Application to high-dimensional equity returns

We compare BCP, GFT, LS, and InvC using a high-dimensional panel of idiosyncratic daily stock returns. We choose GFT, LS, and InvC as benchmarks because, like BCP, they are permutation-equivariant, so the comparison does not depend on the ordering of the stocks. We first remove the Fama–French five factors (FF5) and momentum, then standardize each stock's residuals by its fitted conditional volatility. Our focus is on how the transformed coordinates represent the approximate sparsity pattern and entry magnitudes of the resulting shock correlation matrix.

8.1 Data, factor adjustment, and volatility standardization

We use daily equity price returns from CRSP for the period from January 3, 2011 through December 31, 2025. The six predictors are the market excess return, SMB, HML, RMW, and CMA from FF5 (Fama & French, 2015), together with momentum. We retain all securities with finite returns on all $T = 3{,}772$ trading dates. Of 8,670 candidates, 1,765 form a balanced panel and 6,905 are excluded for incomplete returns. The requirement of a complete 15-year history selects continuously observed securities, to which the empirical findings pertain. For

each security i, we estimate an ordinary least-squares regression over the full period,

$$r_{it} = \mu_i + \vartheta_i' f_t + u_{it}, \qquad f_t = (\mathrm{MKT}_t, \mathrm{SMB}_t, \mathrm{HML}_t, \mathrm{RMW}_t, \mathrm{CMA}_t, \mathrm{Mom}_t)'.$$

For each stock, we fit a zero-mean GJR-GARCH(1,1) model to the OLS residuals (Glosten et al., 1993). Writing u_{it} and h_{it} for the fitted residuals and conditional variances, we form standardized shocks $z_{it} = u_{it}/\sqrt{h_{it}}$ and compute their sample Pearson correlation matrix $\hat{C}$. This baseline is positive definite and uses no shrinkage or entrywise thresholding. We compute the BCP matrix $\hat{B} = B(\hat{C})$ and the GFT, LS, and InvC coordinates from the same $\hat{C}$. Supplementary Section S8 gives estimation and reconstruction details.

8.2 Visual comparison of transformed coordinates

In Figure 1, stocks are ordered by their final available eight-digit GICS subindustry code within the estimation period. Every panel uses the same fixed ordering; strips and boundaries identify the broader GICS sectors. The standardized-shock correlation matrix contains broad regions of weak dependence alongside localized positive blocks and negative bands. BCP retains much of this structure, including the signs and relative magnitudes of the entries. GFT appears substantially paler on the shared scale. The visual pattern of LS is very similar to GFT and is omitted from this figure. InvC displays a different pattern of linear partial association, with prominent negative entries in several positively correlated blocks.

Figure 2 complements the heatmaps by summarizing transformed coordinates conditional on standardized-shock correlations. We estimate the median and the 5th and 95th percentiles using Gaussian weights with bandwidth 0.01, truncated at three bandwidths. The shaded band represents the middle 90% of coordinates, showing their dispersion at each correlation value. Over the displayed range, the BCP conditional median closely follows the 45-degree reference, tracking both the sign and magnitude of shock correlations much more closely than the other medians. The GFT and LS medians are much flatter and closer to the zero-coordinate line, particularly over the negative-correlation range, where they remain nearly constant even as correlations move farther from zero. InvC has a relatively flat, downward-sloping median and a wider band: its coordinates encode scaled negative partial correlations, rather than marginal correlations. Small coordinates under these alternatives can therefore coexist with material marginal correlations.

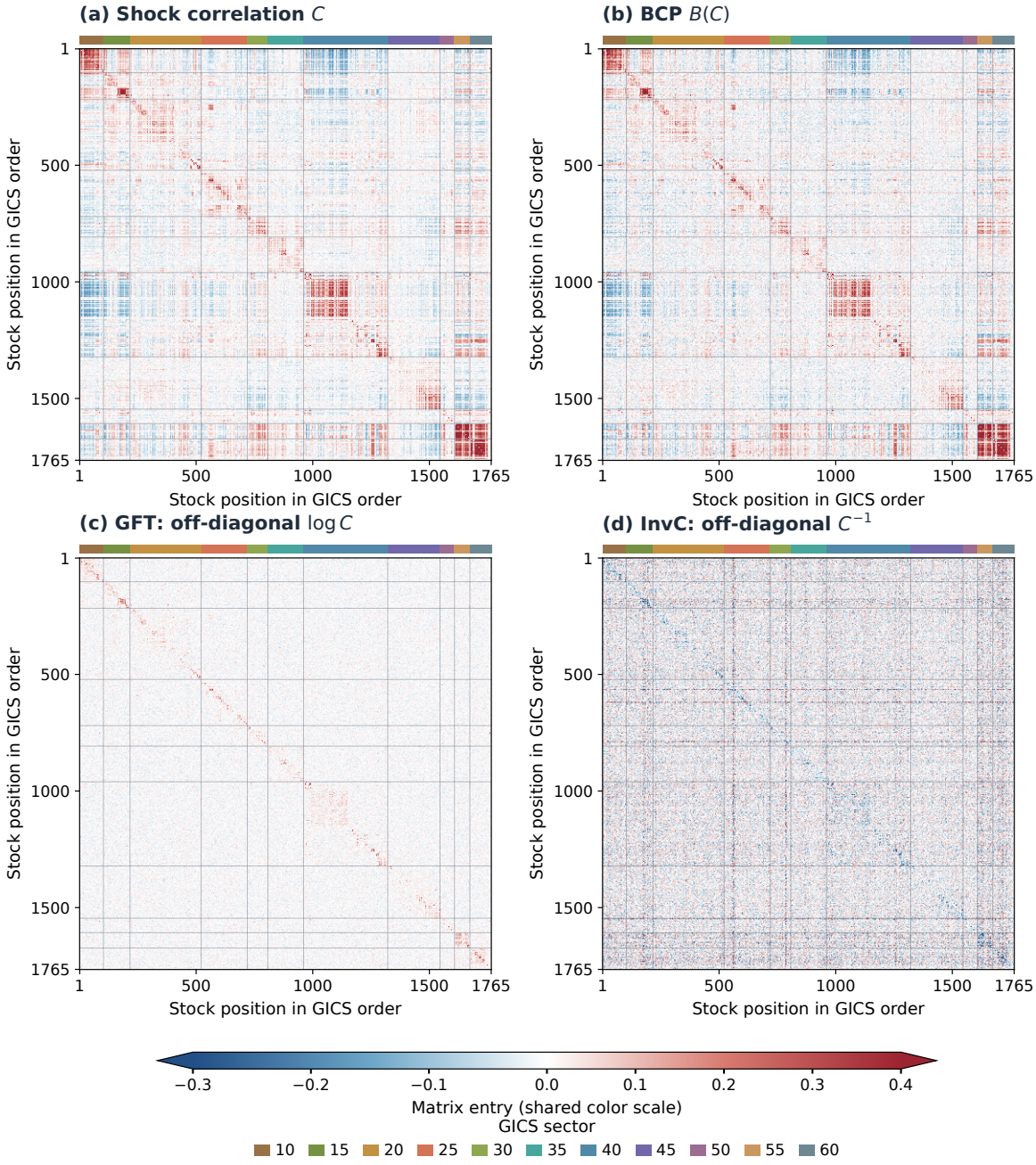

Figure 1: Standardized-shock correlations and transformed coordinates for 1,765 equities, 2011–2025. Each stock's raw daily price return is regressed on an intercept, FF5, and momentum over 3,772 common dates; its residuals are then standardized using a fitted GJR-GARCH(1,1) model. Panels show the shock correlation matrix, BCP, GFT, and InvC in the same GICS order. The shared color scale is $[-0.3, 0.4]$, centered at white for zero, with saturated tails. All four panel diagonals are masked only for display. No matrix entries are thresholded. The visual pattern of LS, omitted here, is very similar to GFT.

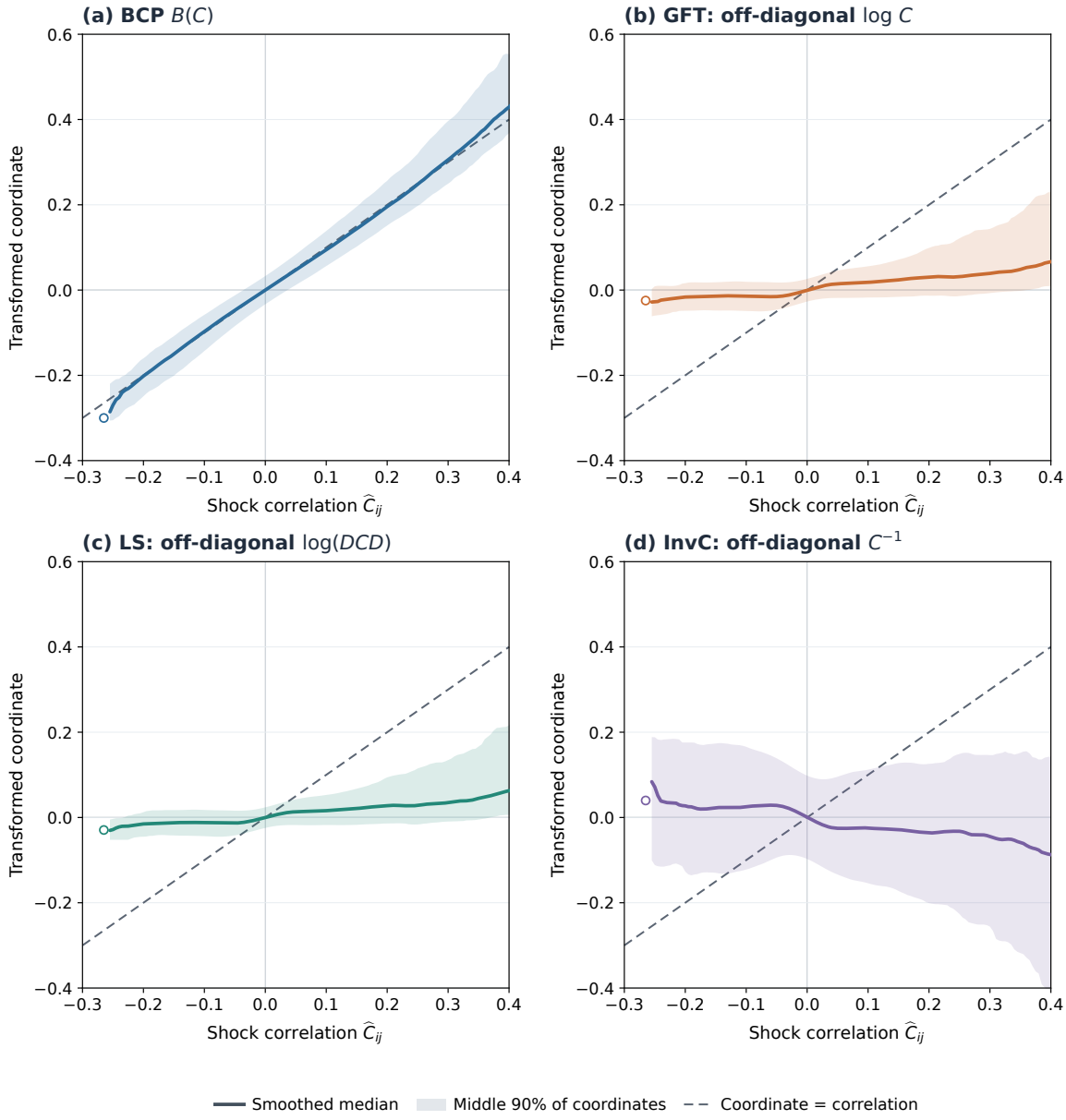

Figure 2: Transformed coordinates conditional on standardized-shock correlations, 2011–2025. The sample correlation matrix $\hat{C}$ has dimension $1{,}765 \times 1{,}765$, giving 1,556,730 unique off-diagonal pairs $i < j$. The horizontal axis shows the shock correlations $\hat{C}_{ij}$, and the vertical axis shows the corresponding off-diagonal coordinates under BCP, GFT, LS, and InvC in panels (a)–(d), respectively. Solid curves are Gaussian-kernel weighted medians; shading spans the corresponding 5th–95th percentiles of coordinates, not confidence intervals. The dashed line is the 45-degree reference. Hollow markers show original bin medians in sparsely populated tails. The displayed range excludes 3,097 pairs (0.20%), all with correlations above 0.4.

8.3 Numerical comparison of sparse reconstructions

We next examine whether this close correspondence translates into accurate correlation reconstructions when a common set of coordinates is set to zero. We select this set using two-sided 5% tests of the original sample correlations. Standard errors use their estimated influence functions, accounting for sample centering and scaling of the fitted shocks, with the Bartlett HAC estimator of Newey & West (1987) and nine lags. The OLS and volatility filters are treated as fixed in these tests. The tests are pointwise, without a multiplicity adjustment; an insignificant estimate does not establish a population zero. For each insignificant $\hat{C}_{ij}$, we set the corresponding coordinate to zero in all four transformations and recover a correlation matrix through each inverse map. For BCP, we set $\tilde{C}_{\mathrm{BCP}} = C(\tilde{B})$, where the sparse coordinate matrix is defined by

$$\tilde{B}_{ij} = \hat{B}_{ij}\, \mathbb{1}\left\{ |\hat{C}_{ij}| > z_{0.975} \times \mathrm{se}(\hat{C}_{ij}) \right\}, \qquad i \neq j,$$

where $z_{0.975}$ is the standard normal 97.5th percentile. The same correlation-based indicator selects the retained GFT, LS, and InvC coordinates. All four methods therefore set the same 67.89% of coordinates to zero. The comparison isolates how these common zero restrictions translate through the inverse maps, rather than selecting a separate specification for each method.

Let $\hat{C}_{0.05}$ denote the reference obtained by setting insignificant entries of $\hat{C}$ directly to zero. Although $\hat{C}$ is positive definite, direct thresholding need not preserve this property (Bickel & Levina, 2008; Guillot & Rajaratnam, 2012). Here it produces an indefinite matrix, with smallest eigenvalue -0.6356. In contrast, each of the four inverse maps yields a positive-definite correlation matrix after coordinate thresholding. The relevant question is therefore how closely these valid reconstructions preserve the original correlations and approximate the desired sparse pattern. Exact zeros in coordinates need not yield exact correlation zeros, and $\hat{C}_{0.05}$ serves only as an entrywise reference.

Table 2 shows that BCP reconstructs the original correlations and approximates the thresholded reference most closely. Among the four sparse reconstructions, it has the highest off-diagonal Pearson correlation and the lowest RMSE relative to both references. Pearson correlation measures agreement in the cross-sectional pattern, whereas RMSE also captures differences in entry magnitudes. BCP is closer to $\hat{C}_{0.05}$ in RMSE than the original $\hat{C}$ is, so the restrictions move the estimate toward the desired sparse pattern while preserving positive definiteness. GFT and LS depart more from both references, and InvC departs the most. Thus, although all four inverse maps yield valid correlation matrices, identical coordinate zeros have markedly different effects on marginal correlations. BCP's closer reconstruction is

Table 2: Correlation reconstruction under common coordinate-zero restrictions.

Statistic	Original	BCP	GFT	LS	InvC
Retained coordinates k	1,556,730	499,883	499,883	499,883	499,883
Coordinates set to zero		67.89%	67.89%	67.89%	67.89%
Pearson correlation with $\hat{C}$	1.0000	0.9747	0.6985	0.6688	0.4758
Pearson correlation with $\hat{C}_{0.05}$	0.9624	0.9883	0.6532	0.6275	0.4218
Off-diagonal RMSE versus $\hat{C}$	0.0000	0.0125	0.1978	0.1856	0.6126
Off-diagonal RMSE versus $\hat{C}_{0.05}$	0.0150	0.0087	0.2017	0.1892	0.6164
Gaussian log-likelihood ($\times 10^3$)	-7,520	-8,332	-8,740	-9,075	-20,619
BIC* ($\times 10^3$)	27,859	**20,781**	21,596	22,268	45,356

Notes: Original denotes the sample correlation $\hat{C}$ of the GJR-GARCH standardized shocks for 2011–2025. The other columns report reconstructions under the common 5% restrictions. Pearson correlations and RMSE use all unique off-diagonal pairs, including zeros; $\hat{C}_{0.05}$ is the directly thresholded reference. *BIC is the descriptive plug-in score $-2\ell + k \log T$, with $T = 3{,}772$; the sparse estimates are not maximum-likelihood refits. Log-likelihood and BIC are in thousands; the lowest BIC is bold.

consistent with the closer correspondence in Figure 2.

The Gaussian working likelihood also favors BCP among the sparse reconstructions. We compute descriptive plug-in BIC scores, counting retained off-diagonal coordinates as parameters. All four sparse estimates have the same parameter count and hence the same BIC penalty, so BCP's higher working likelihood gives it the lowest BIC. The original sample correlation fits best but has a higher BIC than BCP because of its larger parameter count. These scores are descriptive: the sparse estimates are not refitted by maximum likelihood, and the criterion does not adjust for selection of the zero restrictions or serial dependence.

9 Conclusion

BCP is a global real-analytic parametrization of positive-definite correlation matrices by unrestricted coordinates. Its central advantage is that both the transformation and its inverse are available in closed form and require no iterative scaling or diagonal completion. Balancing makes the complete transformed matrix hollow. The rigidity theorem shows that, for dimensions three and higher, direct hollowness and unit local normalization uniquely determine BCP within the class of primary spectral transformations of balanced representatives.

The coordinates combine marginal and partial correlations, respect variable symmetries, preserve block structure, and express normalized correlation inversion as sign reversal. Reduced block formulas and simplified expressions for arrowhead, Gaussian-tree, moving-average, autoregressive, and factor-model correlation matrices facilitate evaluation for familiar dependence structures. Explicit derivatives support estimation and inference.

A further contribution is asymptotic preservation of marginal-correlation sparsity. Under diverging strength of the weakest factor direction and diagonal residual covariance with variances bounded away from zero, BCP coordinates uniformly approximate positively rescaled correlations. This yields support recovery when the smallest nonzero signals dominate approximation and estimation errors, a general coordinate-thresholding guarantee not shared by GFT, LS, or InvC under the same factor assumptions. With a bounded number of factors and heterogeneous loadings, zeroing coordinates at population correlation zeros also yields uniformly accurate reconstruction at the same asymptotic rate. The equity-return illustration complements these results, showing that BCP retains correlation magnitudes and supports accurate positive-definite reconstructions.

These results motivate further work on dynamic correlation models and sparse estimation in BCP coordinates. The unrestricted parametrization and explicit inverse allow correlation dynamics and regularization to be specified while maintaining positive definiteness. Developing estimation procedures and studying their statistical properties are natural next steps, including data-driven threshold selection and more general reconstruction guarantees.

Use of AI tools

During the preparation of this work, the authors used generative AI tools to assist with manuscript review, copy-editing, and numerical checks of mathematical derivations. The authors reviewed and revised the AI-assisted material and take full responsibility for the final manuscript.

References

Aielli, G. P. (2013). Dynamic conditional correlation: on properties and estimation. *Journal of Business and Economic Statistics*, 31, 282–299.

Améndola, C. & Zwiernik, P. (2021). Likelihood geometry of correlation models. *Le Matematiche*, 76, 559–583.

Archakov, I. & Hansen, P. R. (2021). A new parametrization of correlation matrices. *Econometrica*, 89, 1699–1715.

Archakov, I. & Hansen, P. R. (2024). A canonical representation of block matrices with applications to covariance and correlation matrices. *Review of Economics and Statistics*, 106, 1099–1113.

Archakov, I., Hansen, P. R., & Lunde, A. (2026). A multivariate Realized GARCH model. *Journal of Econometrics*, 254, 106040.

Battey, H. (2017). Eigen structure of a new class of covariance and inverse covariance matrices. *Bernoulli*, 23, 3166–3177.

Battey, H. S. (2019). On sparsity scales and covariance matrix transformations. *Biometrika*, 106, 605–617.

Bhatia, R. (1997). *Matrix Analysis*. Graduate Texts in Mathematics 169. Springer.

Bickel, P. J. & Levina, E. (2008). Covariance regularization by thresholding. *Annals of Statistics*, 36, 2577–2604.

Böhm, W. & Hornik, K. (2014). Generating random correlation matrices by the simple rejection method: Why it does not work. *Statistics & Probability Letters*, 87, 27–30.

Chaudhuri, S., Drton, M., & Richardson, T. S. (2007). Estimation of a covariance matrix with zeros. *Biometrika*, 94, 199–216.

Chiu, T. Y. M., Leonard, T., & Tsui, K.-W. (1996). The matrix-logarithmic covariance model. *Journal of the American Statistical Association*, 91, 198–210.

Chudik, A., Pesaran, M. H., & Tosetti, E. (2011). Weak and strong cross-section dependence and estimation of large panels. *The Econometrics Journal*, 14, C45–C90.

Creal, D., Koopman, S. J., & Lucas, A. (2011). A dynamic multivariate heavy-tailed model for time-varying volatilities and correlations. *Journal of Business and Economic Statistics*, 29, 552–563.

Creal, D. & Tsay, R. S. (2015). High dimensional dynamic stochastic copula models. *Journal of Econometrics*, 189, 335–345.

Daniels, M. J. & Pourahmadi, M. (2009). Modeling covariance matrices via partial autocorrelations. *Journal of Multivariate Analysis*, 100, 2352–2363.

David, P. & Gu, W. (2019). A Riemannian structure for correlation matrices. *Operators and Matrices*, 13, 607–627.

Dempster, A. P. (1972). Covariance selection. *Biometrics*, 28, 157–175.

Engle, R. & Kelly, B. (2012). Dynamic equicorrelation. *Journal of Business and Economic Statistics*, 30, 212–228.

Engle, R. F. (2002). Dynamic conditional correlation: A simple class of multivariate generalized autoregressive conditional heteroskedasticity models. *Journal of Business and Economic Statistics*, 20, 339–350.

Engle, R. F., Ledoit, O., & Wolf, M. (2019). Large dynamic covariance matrices. *Journal of Business and Economic Statistics*, 37, 363–375.

Fama, E. F. & French, K. R. (2015). A five-factor asset pricing model. *Journal of Financial Economics*, 116, 1–22.

Fiedler, M. (1964). Relations between the diagonal elements of two mutually inverse positive definite matrices. *Czechoslovak Mathematical Journal*, 14, 39–51.

Forrester, P. J. & Zhang, J. (2020). Parametrising correlation matrices. *Journal of Multivariate Analysis*, 178, 104619.

Glosten, L. R., Jagannathan, R., & Runkle, D. E. (1993). On the relation between the expected value and the volatility of the nominal excess return on stocks. *Journal of Finance*, 48, 1779–1801.

Guillot, D. & Rajaratnam, B. (2012). Retaining positive definiteness in thresholded matrices. *Linear Algebra and its Applications*, 436, 4143–4160.

Hafner, C. M. & Wang, L. (2023). A dynamic conditional score model for the log correlation matrix. *Journal of Econometrics*, 237, 105176.

Hamilton, J. D. (1994). *Time Series Analysis*. Princeton N.J.: Princeton University Press.

Hansen, P. R. (2026). Correlation matrices in high dimensions: Volume, spectrum, and extremes. *arXiv:2608.04162*.

Hero, A. O. & Rajaratnam, B. (2011). Large-scale correlation screening. *Journal of the American Statistical Association*, 106, 1540–1552.

Hero, A. O. & Rajaratnam, B. (2012). Hub discovery in partial correlation graphs. *IEEE Transactions on Information Theory*, 58, 6064–6078.

Higham, N. J. (2008). *Functions of Matrices: Theory and Computation*. Philadelphia, PA: SIAM.

Højsgaard, S. & Lauritzen, S. L. (2008). Graphical Gaussian models with edge and vertex symmetries. *Journal of the Royal Statistical Society, Series B*, 70, 1005–1027.

Huang, K., Ye, X., & Wang, M. (2025). A special Cholesky-based parameterization for estimation of restricted correlation matrices. *Journal of Choice Modelling*, 57, 100580.

Joe, H. (2006). Generating random correlation matrices based on partial correlations. *Journal of Multivariate Analysis*, 97, 2177–2189.

Johnson, C. R. & Reams, R. (2009). Scaling of symmetric matrices by positive diagonal congruence. *Linear and Multilinear Algebra*, 57, 123–140.

Kurowicka, D. & Cooke, R. (2003). A parameterization of positive definite matrices in terms of partial correlation vines. *Linear Algebra and Its Applications*, 372, 225–251.

Leonard, T. & Hsu, J. S. J. (1992). Bayesian inference for a covariance matrix. *Annals of Statistics*, 20, 1669–1696.

Lewandowski, D., Kurowicka, D., & Joe, H. (2009). Generating random correlation matrices based on vines and extended onion method. *Journal of Multivariate Analysis*, 100, 1989–2001.

Lucchetti, R. & Pedini, L. (2024). The spherical parametrisation for correlation matrices and its computational advantages. *Computational Economics*, 64, 1023–1046.

Marshall, A. W. & Olkin, I. (1968). Scaling of matrices to achieve specified row and column sums. *Numerische Mathematik*, 12, 83–90.

Muirhead, R. J. (1982). *Aspects of Multivariate Statistical Theory*. New York: John Wiley & Sons.

Newey, W. K. & West, K. D. (1987). A simple, positive semi-definite, heteroskedasticity and autocorrelation consistent covariance matrix. *Econometrica*, 55, 703–708.

Oh, D. H. & Patton, A. J. (2018). Time-varying systemic risk: Evidence from a dynamic copula model of CDS spreads. *Journal of Business and Economic Statistics*, 36, 181–195.

Oh, D. H. & Patton, A. J. (2023). Dynamic factor copula models with estimated cluster assignments. *Journal of Econometrics*, 237, 105374.

O'Leary, D. P. & Stewart, G. W. (1990). Computing the eigenvalues and eigenvectors of symmetric arrowhead matrices. *Journal of Computational Physics*, 90, 497–505.

Opschoor, A., Lucas, A., Barra, I., & van Dijk, D. (2021). Closed-form multi-factor copula models with observation-driven dynamic factor loadings. *Journal of Business and Economic Statistics*, 39, 1066–1079.

Pakel, C., Shephard, N., Sheppard, K., & Engle, R. F. (2021). Fitting vast dimensional time-varying covariance models. *Journal of Business and Economic Statistics*, 39, 652–668.

Pavlov, D. (2024). Logarithmically sparse symmetric matrices. *Beiträge zur Algebra und Geometrie*, 65, 907–922.

Pinheiro, J. C. & Bates, D. M. (1996). Unconstrained parametrizations for variance-covariance matrices. *Statistics and Computing*, 6, 289–296.

Pourahmadi, M. (1999). Joint mean-covariance models with applications to longitudinal data: unconstrained parameterisation. *Biometrika*, 86, 677–690.

Pourahmadi, M. & Wang, X. (2015). Distribution of random correlation matrices: Hyperspherical parameterization of the Cholesky factor. *Statistics & Probability Letters*, 106, 5–12.

Rapisarda, F., Brigo, D., & Mercurio, F. (2007). Parameterizing correlations: A geometric interpretation. *IMA Journal of Management Mathematics*, 18, 55–73.

Rybak, J. & Battey, H. S. (2021). Sparsity induced by covariance transformation: some deterministic and probabilistic results. *Proceedings of the Royal Society A: Mathematical, Physical and Engineering Sciences*, 477, 20200756.

Rybak, J., Battey, H. S., & Bharath, K. (2026). Regression graphs and sparsity-inducing reparameterizations. *Biometrika*, 113, asaf071.

Saxena, S., Bhat, C. R., & Pinjari, A. R. (2023). Separation-based parameterization strategies for estimation of restricted covariance matrices in multivariate model systems. *Journal of Choice Modelling*, 47, 100411.

Sturmfels, B., Tsukerman, E., & Williams, L. (2016). Symmetric matrices, Catalan paths, and correlations. *Journal of Combinatorial Theory, Series A*, 144, 496–510.

Thanwerdas, Y. (2024). Permutation-invariant log-Euclidean geometries on full-rank correlation matrices. *SIAM Journal on Matrix Analysis and Applications*, 45, 930–953.

Thanwerdas, Y. & Pennec, X. (2022). Theoretically and computationally convenient geometries on full-rank correlation matrices. *SIAM Journal on Matrix Analysis and Applications*, 43, 1851–1872.

Tong, C. & Hansen, P. R. (2023). Characterizing correlation matrices that admit a clustered factor representation. *Economics Letters*, 233, 111433.

Tong, C. & Hansen, P. R. (2026). Dynamic factor correlations. *Journal of Applied Econometrics*, 41, 580–596.

Tong, C., Hansen, P. R., & Archakov, I. (2026). Cluster GARCH. *Journal of Business and Economic Statistics*, 44, 148–161.

Tsay, R. S. & Pourahmadi, M. (2017). Modelling structured correlation matrices. *Biometrika*, 104, 237–242.

Tse, Y. K. & Tsui, A. K. C. (2002). A Multivariate Generalized Autoregressive Conditional Heteroscedasticity Model with Time-Varying Correlations. *Journal of Business and Economic Statistics*, 20, 351–362.

van Oest, R. (2021). Unconstrained Cholesky-based parametrization of correlation matrices. *Communications in Statistics—Simulation and Computation*, 50, 3607–3613.

Wei, Y., Rajaratnam, B., & Hero, A. O. (2023). A unified framework for correlation mining in ultra-high dimension. *IEEE Transactions on Information Theory*, 69, 334–382.

Zwiernik, P. (2025). Entropic covariance models. *Annals of Statistics*, 53, 1371–1405.

Supplement to

A Balanced Parametrization of Correlation Matrices

Peter Reinhard Hansen[§] and Chen Tong[‡]

[§]Department of Economics, University of North Carolina at Chapel Hill

[‡]School of Economics, Xiamen University

October 2026

This supplement provides proofs, extensions, and computational details for the main paper. Notation follows Section 2.1, with additional conventions in Section S1. References without an S prefix refer to the main paper's sections, results, equations, figures, and tables; the S prefix identifies material in this supplement.

S1 Notation and preliminaries

We retain the notation of Section 2.1. For square matrices, $\operatorname{diag}(X_1, \ldots, X_k)$ denotes block-diagonal assembly. The Frobenius inner product is $\langle X, Y \rangle_F = \operatorname{tr}(X'Y)$, and adjoints are taken with respect to this inner product.

The open elliptope $\mathcal{C}_n$ has tangent space $\mathbb{H}_n$ at every point. Correlation normalization identifies matrices that differ by positive diagonal rescaling, giving $\mathcal{C}_n \simeq \mathbb{S}_n^{++} / \operatorname{Diag}^+(n)$, where $\operatorname{Diag}^+(n)$ is the group of positive diagonal matrices acting by $\Sigma \mapsto \Delta\Sigma\Delta$ (David & Gu, 2019; Thanwerdas, 2024).

S2 Proofs for the main results

This section proves the construction, structural, differential, and structured-matrix results in the main paper. The proofs follow the order of the corresponding results. The local expansions are given in Section S4.2.

S2.1 Balancing and spectral characterization

Proof of Theorem 1. Let $\Delta = \mathrm{diag}(\delta_1, \ldots, \delta_n)$ and $A = \Delta C \Delta$. Since $C_{ii} = 1$, $A_{ii} = \delta_i^2$ and $(A^{-1})_{ii} = \delta_i^{-2}(C^{-1})_{ii}$. Condition (1) is therefore equivalent to $\delta_i^4 = (C^{-1})_{ii}$ for $i = 1, \ldots, n$. Moreover,

$$\sum_{i=1}^{n} \left[\log A_{ii} - \log(A^{-1})_{ii}\right]^2 = \sum_{i=1}^{n} \left[4 \log \delta_i - \log\{(C^{-1})_{ii}\}\right]^2,$$

so the same equations give the unique minimizer of the primal–dual discrepancy displayed above. The corresponding general componentwise scaling appears in the proof of Lemma 2.4 of Fiedler (1964, pp. 41–42); here we use only its correlation-matrix specialization. Positivity selects the unique solution $\delta_i = \{(C^{-1})_{ii}\}^{1/4}$, which proves (2); direct substitution gives (3). A signed permutation only permutes the diagonal entries of C^{-1}, because its sign factors cancel on the diagonal, which proves the first identity in (4).

Finally, $\mathcal{I}(C) = D^{-1/2} C^{-1} D^{-1/2}$ and $\mathcal{I}(C)^{-1} = D^{1/2} C D^{1/2}$. The latter matrix has diagonal D. Applying (2) to $\mathcal{I}(C)$ yields $A_{\mathcal{I}(C)} = D^{-1/4} C^{-1} D^{-1/4} = A_C^{-1}$, and proves (4). □

Proof of Theorem 2. Let $m = n - 1$ and $P = \iota_n \iota_n' / n$. For $t \in \mathbb{R}$, define $B_t = -mtP + t(I_n - P) = tI_n - ntP$. The matrix B_t is hollow. Its eigenvalue on the span of ι_n is $-mt$, and its eigenvalue on the orthogonal complement is t, with multiplicity m. Set $A_t = B_t + \sqrt{I_n + B_t^2}$. Then $A_t \succ 0$ and $A_t^{-1} = \sqrt{I_n + B_t^2} - B_t$. Consequently, $\mathrm{Diag}(A_t) - \mathrm{Diag}(A_t^{-1}) = 2\,\mathrm{Diag}(B_t) = 0$, so $A_t \in \mathbb{B}_n$.

Let $r(t) = t + \sqrt{1 + t^2}$ and $f(t) = g\{r(t)\}$. The spectral projectors of B_t give $g(A_t) = f(-mt)P + f(t)(I_n - P)$. Every diagonal entry of this matrix equals $\{f(-mt) + mf(t)\}/n$. Assumption (5) therefore implies

$$f(-mt) + mf(t) = 0, \qquad t \in \mathbb{R}. \tag{S.1}$$

In particular, $f(0) = 0$. Replacing t by $-mt$ in (S.1) and applying that identity once more gives $f(m^2 t) = m^2 f(t)$. For $t \neq 0$ and every positive integer k, $\frac{f(t)}{t} = \frac{f(t/m^{2k})}{t/m^{2k}}$. Because $n \geq 3$, we have $m > 1$, so the argument on the right converges to zero. The function r satisfies $r(0) = 1$ and $r'(0) = 1$; differentiability of g at 1 therefore gives $f'(0) = g'(1)$. Letting $k \to \infty$ yields $f(t) = g'(1)t$ for every t, including $t = 0$.

Finally, r is a bijection from $\mathbb{R}$ onto $(0, \infty)$ with $r^{-1}(a) = (a - a^{-1})/2$. Hence $g(a) = f\{r^{-1}(a)\} = \frac{g'(1)}{2}(a - a^{-1})$, which proves the theorem. □

Remark S1 (Scope of the characterization). For $\kappa > 0$, the scalar map $\phi_\kappa(x) = \sinh\{\kappa \,\mathrm{arsinh}(x)\}/\kappa$ is an odd analytic diffeomorphism with $\phi_\kappa'(0) = 1$. Applied entrywise to $B(C)$, it preserves signed-permutation equivariance, inverse consistency, and block

patterns, and has an explicit inverse. For $\kappa \neq 1$ it lies outside the primary spectral class in Theorem 2. Thus that theorem does not assert uniqueness among all parametrizations with these operational properties.

Within the affine class $\varphi(A) = \alpha A + \beta A^{-1} + \gamma I_n$, the identity $\varphi(A^{-1}) = -\varphi(A)$ for every SPD matrix A forces $\beta = -\alpha$ and $\gamma = 0$. Unit local normalization then gives $\alpha - \beta = 1$, so $\varphi(A) = (A - A^{-1})/2$. The rigidity theorem does not assume this affine form.

S2.2 Proof of the global diffeomorphism

Proof of Theorem 3. For $C \in \mathcal{C}_n$, its balanced representative $A = A_C$ satisfies $\mathrm{Cor}(A) = C$ and $\mathrm{Diag}(A) = \mathrm{Diag}(A^{-1})$. Hence $B = (A - A^{-1})/2$ is symmetric and hollow, and

$$I_n + B^2 = \tfrac{1}{4}(A + A^{-1})^2, \qquad B + \sqrt{I_n + B^2} = A,$$

because $A + A^{-1} \succ 0$. Correlation normalization gives $C\{B(C)\} = C$.

Conversely, for $B \in \mathbb{H}_n$, set $H = \sqrt{I_n + B^2}$ and $A = H + B$. Spectral calculus gives $A \succ 0$ and $A^{-1} = H - B$, so $\mathrm{Diag}(A) = \mathrm{Diag}(A^{-1}) =: E$. For $C = E^{-1/2} A E^{-1/2}$,

$$C^{-1} = E^{1/2} A^{-1} E^{1/2}, \qquad D = E^2, \qquad A_C = D^{1/4} C D^{1/4} = A.$$

Thus $B\{C(B)\} = (A - A^{-1})/2 = B$. The same identities establish the balanced-to-hollow bijection.

Inversion, positive diagonal powers, the principal square root on the positive-definite cone, and correlation normalization are real analytic (Higham, 2008). Both maps are compositions of these operations on the stated domains, completing the proof. □

S2.3 Structural properties

Proof of Theorem 4. Since $(QCQ')^{-1} = QC^{-1}Q'$, the diagonal of the inverse is permuted but unaffected by sign changes. Consequently $\mathrm{Diag}\{(QCQ')^{-1}\}^{1/4} = QD^{1/4}Q'$, where the equality is understood as equality of diagonal matrices after the sign factors cancel. It follows that $A_{QCQ'} = QA_CQ'$. The first identity in (7) follows immediately.

For the inverse, orthogonal functional calculus gives $\sqrt{I_n + (QBQ')^2} = Q\sqrt{I_n + B^2}Q'$. Correlation normalization commutes with signed permutations, yielding the second identity in (7). □

Proof of Theorem 5. Let $K = C^{-1}$ and $D = \mathrm{Diag}(K)$. Then $\mathcal{I}(C) = D^{-1/2}KD^{-1/2}$ and $\mathcal{I}(C)^{-1} = D^{1/2}CD^{1/2}$. Because $\mathrm{Diag}(C) = I_n$, we have $\mathrm{Diag}(\mathcal{I}(C)^{-1}) = D$. Therefore the balanced representative of $\mathcal{I}(C)$ is $A_{\mathcal{I}(C)} = D^{1/4}\mathcal{I}(C)D^{1/4} = D^{-1/4}KD^{-1/4} = A_C^{-1}$. Applying $h(A) = (A - A^{-1})/2$ proves the first identity in (8); the second follows from bijectivity. □

InvC does not share this property. For $C = \frac{1}{2}I_3 + \frac{1}{2}\iota_3\iota_3'$, the off-diagonal entries of C^{-1} are $-1/2$, whereas those of $\mathcal{I}(C)^{-1}$ are $3/4$, not $1/2$.

Proof of Proposition 1. Since $\mathcal{I}(C) = D^{-1/2}C^{-1}D^{-1/2}$, we may rewrite (6) as $B(C) = \frac{1}{2}D^{1/4}\{C - \mathcal{I}(C)\}D^{1/4}$. The off-diagonal entries of $\mathcal{I}(C)$ are $-\pi_{ij}$ and $\sqrt{\tau_i\tau_j} = (K_{ii}K_{jj})^{-1/4}$, which gives (9). □

Proof of Proposition 2. All operations defining D, A_C, $h(A)$, the principal square root, and Cor preserve block diagonal structure. The fixed-point statement follows from Theorem 4 and bijectivity. □

Proof of Proposition 3. Write $D_k = \mathrm{Diag}(C_k^{-1})$ and $A_k = A_{C_k}$. Since $(C_1 \otimes C_2)^{-1} = C_1^{-1} \otimes C_2^{-1}$, $\mathrm{Diag}\{(C_1 \otimes C_2)^{-1}\} = D_1 \otimes D_2$. Positive diagonal powers commute with Kronecker products, and therefore

$$A_{C_1 \otimes C_2} = (D_1^{1/4}C_1D_1^{1/4}) \otimes (D_2^{1/4}C_2D_2^{1/4}) = A_1 \otimes A_2,$$

which proves the first identity in (10). Moreover,

$$S_k = \frac{1}{2}(A_k - A_k^{-1}), \qquad H_k = \frac{1}{2}(A_k + A_k^{-1}) = \sqrt{I_{n_k} + S_k^2}.$$

Hence $A_k = H_k + S_k$ and $A_k^{-1} = H_k - S_k$. Expanding $\frac{1}{2}\{A_1 \otimes A_2 - A_1^{-1} \otimes A_2^{-1}\}$ gives $S_1 \otimes H_2 + H_1 \otimes S_2$, proving the second identity in (10). □

Proof of Proposition 4. Let $\mathcal{H} \subset \mathbb{H}_n$ be compact. Since $B \mapsto C(B)$ is continuous, $C(\mathcal{H}) = \{C(B) : B \in \mathcal{H}\}$ is compact and is contained in $\mathcal{C}_n$. Because $C \mapsto B(C)$ and $B \mapsto C(B)$ are inverse homeomorphisms, $C(\mathcal{H})$ is exactly the inverse image of $\mathcal{H}$ under $C \mapsto B(C)$, proving properness.

For (11), let $A = A_C$ have eigenvalues $a_1, \ldots, a_n$ and set $E = \mathrm{Diag}(A)$. Since $B = \frac{1}{2}(A - A^{-1})$ is a primary matrix function of A, its eigenvalues are $\sinh(\log a_i)$, so

$$\|B\|_2 = \sinh(\log \kappa), \qquad \kappa := \max_i \max\left(a_i, a_i^{-1}\right).$$

For the lower bound, every diagonal entry of A lies between $\lambda_{\min}(A)$ and $\lambda_{\max}(A)$, so for a unit vector x, writing $y = E^{-1/2}x$,

$$x'Cx = y'Ay \geq \lambda_{\min}(A)\,\|y\|^2 \geq \frac{\lambda_{\min}(A)}{\lambda_{\max}(A)}.$$

Hence $\lambda_{\max}(A)/\lambda_{\min}(A) \geq 1/\ell$, and since $\kappa^2 \geq \lambda_{\max}(A)/\lambda_{\min}(A)$ we get $\kappa \geq \ell^{-1/2}$; monotonicity of sinh gives the left inequality, and solving it for ℓ gives (12). For the upper bound, $(C^{-1})_{ii} = (1 - R_i^2)^{-1} \geq 1$ gives $D \succeq I_n$, so $x'Ax = (D^{1/4}x)'C(D^{1/4}x) \geq \ell\,\|x\|^2$ and $\lambda_{\min}(A) \geq \ell$. Also $\lambda_{\max}(A) \leq \lambda_{\max}(C)\max_i (C^{-1})_{ii}^{1/2} \leq n\ell^{-1/2}$, using $\lambda_{\max}(C) \leq \operatorname{tr} C = n$ and $(C^{-1})_{ii} \leq 1/\ell$. Because $\ell \leq 1$, both $n\ell^{-1/2}$ and $1/\ell$ are at most n/ℓ, so $\kappa \leq n/\ell$ and the right inequality follows. Finally, if (13) failed, a bounded subsequence of transformed matrices would have a convergent subsequence. Its image under $B \mapsto C(B)$ would converge to a positive-definite correlation matrix, contradicting $\lambda_{\min}(C_k) \to 0$. The result also follows immediately from the left inequality in (11). □

S2.4 Differentials and inference

Proof of Proposition 5. The inverse differential is $\mathrm{d}K[X] = -KXK$, so $\mathrm{d}D[X] = -\operatorname{Diag}(KXK)$. Because D and Δ are diagonal, $\Delta^{-1}\mathrm{d}\Delta[X] = \frac{1}{4}D^{-1}\mathrm{d}D[X] = U_X$. Differentiating $A = \Delta C \Delta$ therefore gives (14). Finally, $\mathrm{d}(A^{-1})[Z] = -A^{-1}ZA^{-1}$, which gives (15). At $C = I_n$, $K = D = \Delta = A = I_n$ and $\operatorname{diag}(X) = 0$, hence $U_X = 0$ and the result follows. □

Proof of Proposition 6. The derivative of a symmetric matrix function acts on the eigenbasis by the Hadamard product with the matrix of first divided differences (Bhatia, 1997, Theorem V.3.3), so it suffices to identify that matrix. Let $h(a) = (a - a^{-1})/2$, so $B = h(A)$ and $A = f(B)$ with $f = h^{-1}$. For $a_i, a_j > 0$, $h^{[1]}(a_i, a_j) = \frac{1}{2}\left(1 + \frac{1}{a_i a_j}\right)$. The divided difference of the inverse function is therefore

$$f^{[1]}(\lambda_i, \lambda_j) = \{h^{[1]}(a_i, a_j)\}^{-1} = \frac{2a_i a_j}{1 + a_i a_j},$$

including the repeated-eigenvalue case by continuity. This proves (18). Differentiating $C = RAR$ with $R = \operatorname{diag}\{\operatorname{diag}(A)^{-1/2}\}$ gives (19). Since $a_i a_j > 0$, the bound $0 < \Omega_{ij} < 2$ is immediate. □

Proof of Proposition 7. Let $A = B + \sqrt{I_n + B^2}$ and $e = \operatorname{diag}(A)$. The derivative of this spectral lift on $\mathbb{S}_n$ is

$$\mathcal{L}(Y) = Q\{\Omega \circ (Q'YQ)\}Q', \qquad \mathcal{L}^{-1}(Z) = \tfrac{1}{2}(Z + A^{-1}ZA^{-1}).$$

In an eigenbasis of A, the diagonal and symmetric off-diagonal basis elements have multipliers Ω_{ii} and Ω_{ij}, respectively. Hence $\det \mathcal{L} = \prod_{i \le j} \Omega_{ij} > 0$.

Define

$$\mathcal{K}_A = \{DA + AD : D \text{ diagonal}\}, \qquad \mathcal{M}(Z) = Z - \tfrac{1}{2}(V_Z A + A V_Z), \quad V_Z = \operatorname{diag}\{\operatorname{diag}(Z) \oslash e\}.$$

Since $\operatorname{diag}(DA + AD) = 2De$ and every $e_i > 0$, $\mathbb{S}_n = \mathbb{H}_n \oplus \mathcal{K}_A$ and $\mathcal{M}$ is the projection onto $\mathbb{H}_n$ along $\mathcal{K}_A$. Let $\mathcal{N}(Z) = Z - \mathcal{M}(Z)$ be the complementary projection. For $Z = DA + AD$, balancing gives

$$\operatorname{diag}\{\mathcal{L}^{-1}(Z)\} = D\{e + \operatorname{diag}(A^{-1})\} = 2De = \operatorname{diag}(Z).$$

The projection $\mathcal{N}$ is determined solely by the diagonal of its argument, so $\mathcal{N}\mathcal{L}^{-1}(Z) = Z$ on $\mathcal{K}_A$. Thus the $\mathcal{K}_A$ diagonal block of $\mathcal{L}^{-1}$, in this direct-sum decomposition, is the identity. The complementary-minor identity for an invertible block matrix therefore yields

$$\det(\mathcal{M}\mathcal{L}|_{\mathbb{H}_n}) = \det \mathcal{L} \, \det(\mathcal{N}\mathcal{L}^{-1}|_{\mathcal{K}_A}) = \det \mathcal{L}.$$

By Proposition 6, the inverse derivative is $Y \mapsto R\mathcal{M}\mathcal{L}(Y)R$, where $R = \operatorname{diag}(e^{-1/2})$. On hollow matrices, the final scaling multiplies coordinate (i, j) by $(e_i e_j)^{-1/2}$. Its determinant is

$$\prod_{i<j} (e_i e_j)^{-1/2} = \prod_i e_i^{-(n-1)/2}.$$

Combining the two determinants proves (20) in vecl coordinates. The forward determinant follows from the chain rule for the inverse maps. □

Proof of Corollary 1. The transformation is differentiable by Theorem 3. Applying the multivariate delta method to $C \mapsto \operatorname{vecl}\{B(C)\}$ gives (21). Equation (16) gives $J_{I_n} = I_d$, which proves the result. □

S2.5 Block-canonical preliminaries

The fixed-point characterization and exact-preservation proof below apply to every partition with $n_k \ge 1$. A singleton block has no off-diagonal entry or contrast space.

Let $\mathfrak{G}_\mathcal{P}$ be the group of block-diagonal permutation matrices $\operatorname{diag}(P_1, \ldots, P_G)$, where P_k independently permutes the n_k variables in block k.

Lemma S1 (Block symmetry as a fixed-point condition)**.** *For a symmetric matrix X, the following are equivalent:*

(i) $PXP' = X$ *for every* $P \in \mathfrak{G}_{\mathcal{P}}$*;*

(ii) every diagonal block has a common diagonal and, when $n_k \geq 2$*, a common off-diagonal entry, while every off-diagonal block has constant entries.*

Consequently, $\mathcal{C}_n^{\mathcal{P}}$ *and* $\mathbb{H}_n^{\mathcal{P}}$ *are the fixed-point sets of* $\mathfrak{G}_{\mathcal{P}}$ *in* $\mathcal{C}_n$ *and* $\mathbb{H}_n$*, respectively.*

For the reduced calculations, the following canonical formulas are written for $n_k \geq 2$; the singleton modifications are given in Section S5. Set

$$v_k = \frac{1}{\sqrt{n_k}} \iota_{n_k}, \qquad P_{[k,l]} = v_k v_l', \qquad P_{[k,k]}^{\perp} = I_{n_k} - P_{[k,k]}.$$

Choose an orthogonal matrix $Q_{\mathcal{P}}$ whose first G columns are the embedded vectors $v_1, \ldots, v_G$ and whose remaining columns are orthonormal within-block contrasts. The canonical representation of Archakov & Hansen (2024) writes a block-symmetric matrix as

$$\begin{aligned} X_{[k,l]} &= a_{kl} P_{[k,l]}, && k \neq l, \\ X_{[k,k]} &= a_{kk} P_{[k,k]} + \lambda_k P_{[k,k]}^{\perp}, && k = 1, \ldots, G, \end{aligned}$$

and hence

$$Q_{\mathcal{P}}' X Q_{\mathcal{P}} = R \oplus \bigoplus_{k=1}^{G} \lambda_k I_{n_k - 1}, \qquad R = (a_{kl})_{k,l=1}^{G}.$$

Whenever a matrix function f is defined,

$$f(X) = Q_{\mathcal{P}} \left\{ f(R) \oplus \bigoplus_{k=1}^{G} f(\lambda_k) I_{n_k - 1} \right\} Q_{\mathcal{P}}'. \tag{S.2}$$

Thus inversion, powers, logarithms, exponentials, and the principal square root preserve the block pattern. These general facts are used only to derive the BCP-specific formulas in Theorems 8 and 9.

Proof of Lemma S1. If X has the stated block form, independent within-block permutations leave it unchanged. Conversely, these permutations act transitively on the diagonal positions of each block and, when $n_k \geq 2$, on its off-diagonal positions. Invariance therefore makes the entries constant within each of these sets. Independent permutations in blocks k and l act transitively on the positions of $X_{[k,l]}$, so that block is constant as well. This includes

singleton blocks, for which the corresponding permutation group is trivial. Intersecting this fixed-point space with $\mathcal{C}_n$ or $\mathbb{H}_n$ gives the stated block classes. □

Proof of Theorem 7. By Theorem 4, both $C \mapsto B(C)$ and $B \mapsto C(B)$ commute with congruence by every $P \in \mathfrak{G}_{\mathcal{P}}$. Hence each map sends the fixed-point set of $\mathfrak{G}_{\mathcal{P}}$ into the corresponding fixed-point set. The characterization in Lemma S1 gives the two block classes. Since the global transformation and its inverse are mutually inverse analytic diffeomorphisms, their restrictions are also mutually inverse analytic diffeomorphisms. The argument imposes no lower bound on block size beyond $n_k \geq 1$. □

Proof of Theorem 8. The canonical representation gives

$$Q'_{\mathcal{P}} C^{-1} Q_{\mathcal{P}} = R^{-1} \oplus \bigoplus_{k=1}^{G} \lambda_k^{-1} I_{n_k - 1}.$$

The diagonal of $(R^{-1})_{kk} P_{[k,k]} + \lambda_k^{-1} P_{[k,k]}^{\perp}$ is constant and equal to δ_k^4 in (24). This proves the asserted blockwise form of D.

Because $D^{1/4}$ is constant within each block, its canonical action is

$$Q'_{\mathcal{P}} D^{1/4} Q_{\mathcal{P}} = \Delta \oplus \bigoplus_{k=1}^{G} \delta_k I_{n_k - 1}.$$

It follows that the balanced representative $A_C = D^{1/4} C D^{1/4}$ has canonical form

$$\Delta R \Delta \oplus \bigoplus_{k=1}^{G} \delta_k^2 \lambda_k I_{n_k - 1},$$

and its inverse has the corresponding form with Δ and δ_k inverted and R and λ_k replaced by their inverses. Taking half their difference gives the two quantities in (25).

The diagonal entries of the kth diagonal block equal $\frac{M_{kk}}{n_k} + \left(1 - \frac{1}{n_k}\right) \zeta_k$. They vanish because B is hollow. Reconstructing the blocks from the projectors gives (26). □

Proof of Theorem 9. By the functional-calculus identity (S.2),

$$B + \sqrt{I_n + B^2} = Q_{\mathcal{P}} \left\{ F \oplus \bigoplus_{k=1}^{G} a_k I_{n_k - 1} \right\} Q'_{\mathcal{P}}.$$

Its diagonal entries in block k equal e_k in (28). Correlation normalization multiplies block (k, l) by $e_k^{-1/2} e_l^{-1/2}$. Expanding the projectors in the canonical representation yields (29). The diagonal entries are one by construction. □

Proof of Corollary 2. The forward formulas in Theorem 8 require the inverse of the $G \times G$ core R and then only diagonal and scalar operations. The inverse formulas in Theorem 9 require one symmetric $G \times G$ eigendecomposition, used to evaluate $F = e^{\operatorname{arsinh} H}$ on the core H of (27), and then only scalar operations. The unrestricted block parameters consist of one value for each unordered pair of blocks and one within-block parameter for every nonsingleton block, giving dimension $G(G-1)/2 + |\{k : n_k > 1\}|$. For singleton blocks, the rules in Section S5 omit the absent contrast terms and retain the same $G \times G$ core calculations and computational cost. □

S2.6 Equicorrelation formulas

Proof of Proposition 8 and identity (32). For $C = (1-\rho)I_n + \rho\iota\iota'$, the inverse is $C^{-1} = \frac{1}{1-\rho}I_n - \frac{\rho}{(1-\rho)\{1+(n-1)\rho\}}\iota\iota'$. Hence $D = \delta^4 I_n$ with $\delta^4 = \frac{1+(n-2)\rho}{(1-\rho)\{1+(n-1)\rho\}}$. Both $A_C = \delta^2 C$ and $A_C^{-1} = \delta^{-2}C^{-1}$ have constant diagonal and constant off-diagonal entries. Their off-diagonal half-difference is

$$b = \frac{1}{2}\left[\rho\delta^2 + \frac{\rho}{(1-\rho)\{1+(n-1)\rho\}\delta^2}\right],$$

which simplifies to (30).

Now $B = b(\iota\iota' - I_n)$ has eigenvalue $(n-1)b$ in the span of ι and eigenvalue $-b$ on its orthogonal complement. Therefore $A = e^{\operatorname{arsinh} B}$ has corresponding eigenvalues $a_1 = e^{\operatorname{arsinh}((n-1)b)}$ and $a_2 = e^{-\operatorname{arsinh}(b)}$. Since $C = \operatorname{Cor}(A)$ and A has a constant diagonal, the ratio of the two distinct eigenvalues of C equals a_1/a_2. But the same ratio is $\frac{1+(n-1)\rho}{1-\rho}$. Taking logarithms gives $\log\frac{1+(n-1)\rho}{1-\rho} = \operatorname{arsinh}((n-1)b) + \operatorname{arsinh}(b)$, which proves (32).

Finally, a matrix with eigenvalues a_1 and a_2 in the two invariant subspaces has correlation coefficient $\rho = \frac{a_1-a_2}{a_1+(n-1)a_2}$, which gives (31). Since the global map is a diffeomorphism and preserves the one-dimensional equicorrelation class, b_n is a smooth bijection onto $\mathbb{R}$; monotonicity also follows directly from the displayed inverse. □

S2.7 BCP for selected structured correlation matrices

Proof of Proposition 9. The Schur complement of (33) gives

$$(C^\star)^{-1} = \omega^{-2}\begin{pmatrix} 1 & -\rho' \\ -\rho & \omega^2 I_r + \rho\rho' \end{pmatrix}, \qquad D_\star = \omega^{-2}\operatorname{diag}(1, R_\rho^4).$$

Substitution into (6) gives the factor-to-leaf entries η_ρ in (34). For distinct leaves j, k, $C^\star_{j+1,k+1} = 0$ and the precision contribution is $-\rho_j\rho_k/(2\omega h_j^{1/4}h_k^{1/4}) = -v_{\rho,j}v_{\rho,k}/(2\omega)$. The diagonal is zero by balancing, proving the lower block and (35). □

Proof of Proposition 10. Choose an arbitrary root and orient every edge away from it. A standardized Gaussian tree can be generated recursively as $X_j = \theta_{ij} X_i + \sqrt{1-\theta_{ij}^2}\,\varepsilon_j$ when i is the parent of j, with independent standard-normal innovations. Iterated conditioning gives the path-product correlation in (36). Expanding the negative Gaussian log density, up to an additive constant,

$$\frac{1}{2}X_{\text{root}}^2 + \frac{1}{2}\sum_{j\neq\text{root}} \frac{(X_j - \theta_{p(j)j}X_{p(j)})^2}{1-\theta_{p(j)j}^2}$$

gives the off-diagonal and diagonal precision entries in (37), independently of the chosen root. Substituting these precision entries and the path-product correlations into (6) proves (38). □

Proof of Proposition 11. Set $\theta_k = 0$ for $k < 0$ or $k > q$ and let $L = (\theta_{i-j})_{i,j=1}^n$. With $\varepsilon = (\varepsilon_1, \ldots, \varepsilon_n)'$ and $\varepsilon_- = (\varepsilon_0, \varepsilon_{-1}, \ldots, \varepsilon_{1-q})'$, the observation vector satisfies

$$x = L\varepsilon + H\varepsilon_-.$$

The innovation vectors have identity covariance matrices and are uncorrelated with one another. Since each x_t has variance s,

$$C = s^{-1}(LL' + HH').$$

The matrix L is unit lower triangular, so this representation proves positive definiteness for every finite n, irrespective of the roots of the MA polynomial. The convolution identity

$$\sum_{\ell=0}^{\min(q,k)} \theta_\ell \psi_{k-\ell} = \mathbb{1}\{k=0\}$$

implied by (40) gives $F = L^{-1}$. Applying the Woodbury identity yields

$$\begin{aligned} C^{-1} &= sF'\left(I_n + FHH'F'\right)^{-1}F \\ &= s\left\{F'F - F'FH\left(I_q + H'F'FH\right)^{-1}H'F'F\right\} \\ &= s\left(W - WHM^{-1}H'W\right). \end{aligned}$$

Here M is positive definite because $W = F'F$ is positive definite. Substituting this precision matrix and $C_{ij} = \rho_{|i-j|}$ into (6) gives (42); its specialization outside the correlation band follows from $\rho_h = 0$ for $h > q$. □

Proof of Proposition 12. Let $x = (x_1, \dots, x_n)'$ and let T be the unit lower-triangular matrix with first p rows E_p and remaining rows $r'_{p+1}, \dots, r'_n$. Then $Tx = (x_1, \dots, x_p, \varepsilon_{p+1}, \dots, \varepsilon_n)'$. Causality and the white-noise assumption imply that the first p components are uncorrelated with the remaining innovations, which are mutually uncorrelated. Hence

$$TCT' = \begin{pmatrix} C_p & 0 \\ 0 & \sigma^2 I_{n-p} \end{pmatrix}, \qquad K = T' \begin{pmatrix} C_p^{-1} & 0 \\ 0 & \sigma^{-2} I_{n-p} \end{pmatrix} T.$$

Expanding the second identity gives (43), without any distributional assumption beyond the stated second moments. The initial-block term is supported on the first p coordinates, and each r_s is supported on $\{s-p, \dots, s\}$. Hence $K_{ij} = 0$ for $|i-j| > p$. Substitution in (6) proves (44).

For completeness, the precision entries have simple scalar expressions away from the boundaries. Put

$$a = 1 + \sum_{\ell=1}^{p} \phi_\ell^2, \qquad g_h = \begin{cases} -\phi_h + \displaystyle\sum_{\ell=1}^{p-h} \phi_\ell \phi_{\ell+h}, & 1 \le h \le p, \\ 0, & h > p. \end{cases}$$

For $p+1 \le i < j \le n-p$, all terms contributing to the interior precision entries are present in the sum in (43), while the initial-block term is zero. Collecting their coefficients gives $K_{ii} = K_{jj} = a/\sigma^2$ and $K_{ij} = g_{j-i}/\sigma^2$. Consequently,

$$[B(C)]_{ij} = \frac{a\rho_h - g_h}{2\sqrt{a\sigma^2}}, \qquad h = j - i, \quad p+1 \le i < j \le n-p. \tag{S.3}$$

Thus the interior entries depend only on the lag, although the full transformed matrix need not be Toeplitz.

For $p = 1$, $C_p = (1)$, $\phi_1 = \rho$, and $\sigma^2 = 1 - \rho^2$. The precision formula gives the endpoint and interior diagonal entries stated in Section 6.4, the adjacent entries $K_{i,i+1} = -\rho/(1-\rho^2)$, and zeros elsewhere off the diagonal. These entries give (45), equivalently obtained from Proposition 10 on a homogeneous path. □

Proof of Proposition 13. The Woodbury identity applied to (46) gives $C^{-1} = Q^{-1} - Q^{-1}\Lambda M^{-1}\Lambda' Q^{-1}$. Its ith diagonal entry is exactly δ_i^4 in (47). For $i \neq j$,

$$C_{ij} = \lambda_i' \lambda_j, \qquad (C^{-1})_{ij} = -\frac{\lambda_i' M^{-1} \lambda_j}{q_i q_j}.$$

Substitution into (6) proves (48). The definitions in (49) give

$$u_i'u_j = \delta_i\delta_j\lambda_i'\lambda_j, \qquad v_i'v_j = \frac{\lambda_i'M^{-1}\lambda_j}{q_iq_j\delta_i\delta_j},$$

which proves (50). When $r = 1$, $M = \kappa$ and direct substitution yields the one-factor formula. □

S3 Adjoint derivative and likelihood scores

The inverse derivative in Proposition 6 gives objective gradients without forming a full Jacobian. For symmetric G_C, set

$$\tilde{G} = RG_CR, \qquad H_G = \tilde{G} - \operatorname{diag}\{\operatorname{diag}(A\tilde{G}) \oslash e\}.$$

Its Frobenius adjoint is

$$(\mathrm{d}_BC)^*[G_C] = \operatorname{Off}\left[Q\{\Omega \circ (Q'H_GQ)\}Q'\right]. \tag{S.4}$$

If $\mathrm{d}\ell = \operatorname{tr}(G_C\mathrm{d}C)$ and $s = \operatorname{vecl}(B)$, then $\partial\ell/\partial s = 2\operatorname{vecl}\{(\mathrm{d}_BC)^*[G_C]\}$; the factor two accounts for the two symmetric entries associated with each coordinate.

Proof. For a symmetric direction Z, put $V = \operatorname{diag}\{\operatorname{diag}(Z) \oslash e\}$. The normalization differential is $\mathrm{d}_A \operatorname{Cor}[Z] = R\{Z - (VA + AV)/2\}R$. Therefore

$$\langle G_C, \mathrm{d}_A \operatorname{Cor}[Z]\rangle_F = \left\langle \tilde{G}, Z\right\rangle_F - \sum_i \frac{(A\tilde{G})_{ii}}{e_i}Z_{ii} = \langle H_G, Z\rangle_F.$$

The spectral derivative $Z \mapsto Q\{\Omega \circ (Q'ZQ)\}Q'$ is self-adjoint. Composing these adjoints and projecting onto the hollow input space gives (S.4). □

S4 Relations to the generalized Fisher transformation

This section complements Section 4.3 with the exact global transition, a commuting-class identity, and the proof of the local comparison.

S4.1 Exact transition and diagonal commutation

Writing $A = B + \sqrt{I_n + B^2} = e^{\operatorname{arsinh} B}$ and $E = \operatorname{Diag}(A)$, the transition from BCP to GFT is the analytic diffeomorphism

$$\mathcal{T}(B) = \operatorname{Off} \log(E^{-1/2} A E^{-1/2}).$$

A diagonal congruence generally does not commute with the matrix logarithm. The following condition gives an exact simplification.

Proposition S1 (Exact link under diagonal commutation)**.** *If $D = \operatorname{Diag}(C^{-1})$ commutes with C, then*

$$\operatorname{Off}(\log C) = \operatorname{Off}\{\operatorname{arsinh} B(C)\}. \tag{S.5}$$

This condition is equivalent to $C_{ij} = 0$ whenever $(C^{-1})_{ii} \neq (C^{-1})_{jj}$, so the class consists of direct sums of blocks with scalar precision diagonals. It includes equicorrelation and symmetric circulant correlation matrices.

Proof. The condition is equivalent to $E = \operatorname{Diag}(A_C) = D^{1/2}$ commuting with A_C. Then $C = E^{-1} A_C$ and $\log C = \log A_C - \log E = \operatorname{arsinh} B(C) - \log E$. Taking off-diagonal entries proves (S.5). □

S4.2 Local expansions

This section proves Theorem 6. Throughout, the dimension n is fixed, so constants in the remainder bounds may depend on n. Let $C = I_n + E$ with $E \in \mathbb{H}_n$, and use a fixed submultiplicative matrix norm, as in the theorem. Write $G_2 = \operatorname{Diag}(E^2)$ and $G_3 = \operatorname{Diag}(E^3)$.

The inverse expansion is $C^{-1} = I_n - E + E^2 - E^3 + \mathcal{O}(\|E\|^4)$. Therefore $D = I_n + G_2 - G_3 + \mathcal{O}(\|E\|^4)$. Because G_2 and G_3 are respectively second and third order,

$$\begin{aligned} D^{1/4} &= I_n + \frac{1}{4} G_2 - \frac{1}{4} G_3 + \mathcal{O}(\|E\|^4), \\ D^{-1/4} &= I_n - \frac{1}{4} G_2 + \frac{1}{4} G_3 + \mathcal{O}(\|E\|^4). \end{aligned}$$

Multiplying out gives

$$\begin{aligned} A_C &= I_n + E + \frac{1}{2} G_2 - \frac{1}{2} G_3 + \frac{1}{4}(G_2 E + E G_2) + \mathcal{O}(\|E\|^4), \\ A_C^{-1} &= I_n - E + E^2 - E^3 - \frac{1}{2} G_2 + \frac{1}{2} G_3 + \frac{1}{4}(G_2 E + E G_2) + \mathcal{O}(\|E\|^4). \end{aligned}$$

Taking half the difference,

$$\begin{aligned} B(I_n + E) &= E - \frac{1}{2}E^2 + \frac{1}{2}E^3 + \frac{1}{2}G_2 - \frac{1}{2}G_3 + \mathcal{O}(\|E\|^4) \\ &= E - \frac{1}{2}\operatorname{Off}(E^2) + \frac{1}{2}\operatorname{Off}(E^3) + \mathcal{O}(\|E\|^4). \end{aligned}$$

The matrix logarithm has expansion $\log(I_n + E) = E - \frac{1}{2}E^2 + \frac{1}{3}E^3 + \mathcal{O}(\|E\|^4)$. Applying Off gives

$$\operatorname{Off}\{\log(I_n + E)\} = E - \frac{1}{2}\operatorname{Off}(E^2) + \frac{1}{3}\operatorname{Off}(E^3) + \mathcal{O}(\|E\|^4).$$

Subtracting proves (22) and Theorem 6.

Finally, let $B = B(I_n + E)$ and $H = \operatorname{Off}\{\log(I_n + E)\}$. Since $E = B + \mathcal{O}(\|B\|^2)$, (22) implies

$$\mathcal{T}(B) = H = B - \frac{1}{6}\operatorname{Off}(B^3) + \mathcal{O}(\|B\|^4).$$

For $E_T = \hat{C}_T - I_n = \mathcal{O}_p(T^{-1/2})$, the cubic difference is $\mathcal{O}_p(T^{-3/2})$ and the fourth-order remainder is $\mathcal{O}_p(T^{-2})$. This gives the local asymptotic equivalence stated in Section 4.3. The maps are analytic, so differentiating their expansions also shows that their Jacobians differ at order $\|E\|^2$.

S5 Block formulas with singleton groups

For a partition with singleton groups, the formulas in Theorems 8 and 9 apply to every nonsingleton block without change. A singleton has no within-block correlation or contrast parameter. For each k with $n_k = 1$, use

$$R_{kk} = 1, \qquad \delta_k^4 = (R^{-1})_{kk}, \qquad H_{kk} = 0, \qquad e_k = F_{kk}.$$

Omit λ_k, ζ_k, a_k, and the formula for ρ_{kk} for that group. The between-block formulas remain

$$\eta_{kl} = \frac{M_{kl}}{\sqrt{n_k n_l}}, \qquad \rho_{kl} = \frac{F_{kl}}{\sqrt{n_k n_l e_k e_l}}, \quad k \neq l.$$

These rules follow from (S.2) by omitting the absent contrast spaces. The number of free block coordinates is $G(G-1)/2 + |\{k : n_k > 1\}|$, and only $G \times G$ matrix functions are needed.

S6 Computational implementation

Forward and inverse maps. When applying the forward transformation to a singular sample correlation matrix, a positive-definite estimator must first be obtained. For the forward map, obtain $K = C^{-1}$ from a Cholesky factorization, set $\delta_i = K_{ii}^{1/4}$, and evaluate $B_{ij} = \frac{1}{2}\{\delta_i\delta_j C_{ij} - K_{ij}/(\delta_i\delta_j)\}$. Set the diagonal to zero to remove roundoff. For the inverse, compute $B = Q\,\mathrm{diag}(\lambda_i)Q'$, evaluate $a_i = \exp\{\mathrm{arsinh}(\lambda_i)\}$, and return $\mathrm{Cor}\{Q\,\mathrm{diag}(a_i)Q'\}$. This avoids cancellation in $\lambda_i + \sqrt{1+\lambda_i^2}$ for large negative λ_i.

Derivative products. Reuse the inverse eigendecomposition in Proposition 6 and (S.4). With $u_i = \mathrm{arsinh}(\lambda_i)$, evaluate the divided differences as

$$\Omega_{ij} = 2\,\mathrm{expit}(u_i + u_j), \qquad \mathrm{expit}(x) = (1+e^{-x})^{-1},$$

using an overflow-safe logistic routine. The derivative and adjoint then require matrix products and diagonal operations, without constructing a $d \times d$ Jacobian. Map-only evaluations do not form Ω.

LS scaling. For the LS forward map, solve $Cx = x^{-1}$ with $x > 0$ and evaluate $\log\{\mathrm{diag}(x)C\,\mathrm{diag}(x)\}$. This positive diagonal scaling to unit row sums exists uniquely (Marshall & Olkin, 1968; Johnson & Reams, 2009). The damped Newton step solves $\{C + \mathrm{diag}(x^{-2})\}s = -(Cx - x^{-1})$, starting from $x = \iota_n$ and restricting the step to preserve positivity (Thanwerdas, 2024, Section 3.5).

InvC inversion. The diagonal-completion formulation follows Améndola & Zwiernik (2021, Section 4.2); its interpretation as unrestricted correlation coordinates is established by Zwiernik (2025, Corollary 5.8). For hollow precision coordinates W, set $K(v) = W + \mathrm{diag}(v)$ and $C = K(v)^{-1}$. Recover the missing diagonal by minimizing $\phi(v) = \iota_n' v - \log\det K(v)$ over $K(v) \succ 0$. Its gradient is $\iota_n - \mathrm{diag}(C)$ and its Hessian is $C \circ C \succ 0$, so the objective is strictly convex with first-order condition $\mathrm{diag}(C) = \iota_n$. With $C^{(k)} = K(v^{(k)})^{-1}$, the Newton step solves

$$(C^{(k)} \circ C^{(k)})s^{(k)} = \mathrm{diag}(C^{(k)}) - \iota_n.$$

Initialize $v_i^{(0)} = 1 + \sum_{j\neq i}|W_{ij}|$, which ensures positive definiteness by strict diagonal dominance. Update $v^{(k+1)} = v^{(k)} + \alpha_k s^{(k)}$, backtracking from $\alpha_k = 1$ to maintain positive definiteness and satisfy Armijo decrease of ϕ. Return $C^{(k)}$ when $\|\,\mathrm{diag}(C^{(k)}) - \iota_n\|_\infty$ is below the chosen tolerance.

S7 Sparsity preservation: proofs and comparisons

This appendix supplies the proofs for Section 7 of the main paper, followed by calculations and counterexamples for GFT, LS, and inverse-correlation (InvC) coordinates. The notation and factor assumptions are those of Assumption 1. No additional conditions are imposed unless stated.

S7.1 Proofs of the BCP results

Proof of Theorem 10. Suppress the subscript n and set $M = I_{r_n} + \Lambda'\Omega^{-1}\Lambda$, so that $M \succeq (1+\mu_n)I_{r_n}$. Woodbury's identity gives

$$K = \Omega^{-1} - \Omega^{-1}\Lambda M^{-1}\Lambda'\Omega^{-1}. \tag{S.6}$$

The loading bound and (51) imply

$$|K_{ij}| \le h_n \quad (i \ne j), \qquad 0 \le \omega_i^{-1} - K_{ii} \le h_n.$$

For a correlation matrix, a Schur complement gives $K_{ii} \ge 1$. Equation (S.6) also gives $K_{ii} \le \omega_i^{-1} \le a^{-1}$. Since the derivative of $x^{1/4}$ is at most $1/4$ on $[1,\infty)$,

$$|\delta_i - \omega_i^{-1/4}| \le h_n/4, \qquad |\delta_i\delta_j - (\omega_i\omega_j)^{-1/4}| \le a^{-1/4}h_n/2.$$

Substitute these inequalities into (52), using $|C_{ij}| \le 1$ and $\delta_i\delta_j \ge 1$. This proves (53)–(54). When $C_{ij} = 0$, only the precision term remains, proving (55). □

Proof of Corollary 3. Null coordinates satisfy (55). On the support, Theorem 10 gives $|B_{ij,n}| \ge m_n/2 - K_a h_n$, and the perturbation is smaller than the positively scaled signal under the displayed conditions. The bounds hold simultaneously over all pairs, proving support and sign recovery. □

Proof of Corollary 4. Write $E_n = \max_{i\ne j}|\hat{B}_{ij,n} - c_n B_{ij,n}|$. At null pairs, $|\hat{B}_{ij,n}| \le c_n h_n/2 + E_n = o_p(\tau_n)$. At nonnull pairs, $|\hat{B}_{ij,n}| \ge c_n(m_n/2 - K_a h_n) - E_n$. Since $c_n^{-1} = O_p(1)$, dividing the threshold and both error terms by $c_n m_n$ gives quantities converging to zero in probability. The lower bound therefore exceeds τ_n simultaneously over the support with probability tending to one. The same bounds make the total perturbation $o_p(c_n m_n)$, proving sign recovery because $c_n > 0$. □

Proof of Proposition 14. Suppress n, write $\mu = \mu_n$ and $r = r_n$, and use $\|H\|_{\max} = \max_{i,j} |H_{ij}|$. Set $K = C^{-1}$, $\Delta = \operatorname{diag}(K_{ii}^{1/4})$, and $W = \Omega^{-1} - K$. By (S.6), $W \succeq 0$, $\operatorname{rank}(W) \le r$, $\|W\|_2 \le a^{-1}$, and $\max_i W_{ii} \le h_n$. Define

$$U = \frac{\Delta\Lambda}{\sqrt{2}}, \qquad R = \frac{1}{2}\Delta^{-1}W\Delta^{-1}, \qquad D_0 = \operatorname{diag}\left(\frac{q_i - q_i^{-1}}{2}\right), \qquad q_i = \omega_i\sqrt{K_{ii}}.$$

Since $1 \le K_{ii} \le \omega_i^{-1}$, we have $a \le q_i \le 1$, so D_0 is uniformly bounded. Direct substitution gives $B = D_0 + UU' + R$. The loading and residual-variance bounds imply

$$\lambda_{\min}(U'U) \ge a\mu/2, \qquad \max_i \|U_{i\cdot}\|_2^2 \le \frac{1-a}{2\sqrt{a}}.$$

Indeed, $U'U \succeq \Lambda'\Lambda/2 \succeq a\Lambda'\Omega^{-1}\Lambda/2$. Moreover, $R \succeq 0$, $\operatorname{rank}(R) \le r$, and

$$\|R\|_2 \le \frac{1}{2a}, \qquad \|R\|_{\max} \le \max_i R_{ii} \le \frac{h_n}{2}, \qquad \max_i \|R_{i\cdot}\|_2^2 \le \|R\|_2 \max_i R_{ii} \le \frac{h_n}{4a}.$$

Let T retain the diagonal of R and its off-diagonal entries wherever $C_{ij} \neq 0$, setting the other entries to zero. At a correlation zero, $(UU')_{ij} = 0$, so $\tilde{B} = D_0 + UU' + T$ exactly. Masking entries cannot increase a row's Euclidean norm or the Frobenius norm. Consequently, for either $J = R$ or $J = T$,

$$\|J\|_{\max} = O(\mu^{-1}), \qquad \max_i \|J_{i\cdot}\|_2 = O(\mu^{-1/2}), \qquad \|J\|_2 = O(1),$$

where the last bound for T follows from $\|T\|_2 \le \|T\|_F \le \|R\|_F \le \sqrt{r}/(2a)$ and $\sup_n r_n < \infty$.

We next establish the entrywise bound needed for the inverse map. Let $X = D_0 + UU' + J$, $L = D_0 + J$, $H = U'U$, and $V = UH^{-1/2}$. Then $V'V = I_r$, $X = L + VHV'$, and $\max_i \|e_i'V\|_2 = O(\mu^{-1/2})$, where e_i is the ith coordinate vector. Choose a fixed $M \ge 1$ with $\|L\|_2, \|D_0\|_2 \le M$. The min–max principle places $n - r$ eigenvalues of X in $[-M, M]$ and its remaining r eigenvalues in $[a\mu/2 - M, \infty)$. For sufficiently large n, the latter interval lies to the right of $M + 1$.

Set $g(z) = \sqrt{1 + z^2} - z$, taking the square-root branch that is positive on the real axis; g is analytic on $|\operatorname{Im} z| < 1$. Let Γ be the positively oriented rectangle with vertical sides $\operatorname{Re} z = \pm(M + 1)$ and horizontal sides $\operatorname{Im} z = \pm 1/2$. On this fixed contour, the resolvents

$$\mathcal{R}(z) = (zI_n - L)^{-1}, \qquad \mathcal{R}_0(z) = (zI_n - D_0)^{-1}$$

are uniformly bounded in spectral norm, and $\mathcal{R}_0(z)$ is diagonal. The resolvent identities

$$\mathcal{R} - \mathcal{R}_0 = \mathcal{R}_0 J \mathcal{R}_0 + \mathcal{R}_0 J \mathcal{R} J \mathcal{R}_0,$$
$$\mathcal{R} V = \mathcal{R}_0 V + \mathcal{R}_0 J \mathcal{R} V$$

and the entrywise and row-norm bounds above yield, uniformly on Γ,

$$\|\mathcal{R} - \mathcal{R}_0\|_{\max} = O(\mu^{-1}), \qquad \max_i \|e_i' \mathcal{R} V\|_2 = O(\mu^{-1/2}).$$

For the quadratic resolvent term, each entry is bounded by a constant times $\|J_{i\cdot}\|_2 \|J_{j\cdot}\|_2$; for the second identity, use $\|\mathcal{R} V\|_2 = O(1)$.

The compression $\mathcal{K}(z) = V' \mathcal{R}(z) V$ is uniformly invertible on Γ. To see this, for every $\lambda \in [-M, M]$, the imaginary part of $(z - \lambda)^{-1}$ has a common sign and magnitude bounded away from zero on either horizontal side. The same is true of its real part on either vertical side. The spectral theorem and $V'V = I_r$ therefore give $|x^* \mathcal{K}(z) x| \geq c \|x\|_2^2$ for all complex x, with a constant $c > 0$ independent of n and $z \in \Gamma$. Since $\|H^{-1}\|_2 = O(\mu^{-1})$, $(H^{-1} - \mathcal{K}(z))^{-1}$ is also uniformly bounded. Woodbury's identity gives

$$(z I_n - X)^{-1} - \mathcal{R}(z) = \mathcal{R}(z) V \{H^{-1} - \mathcal{K}(z)\}^{-1} V' \mathcal{R}(z).$$

The preceding row-norm bound, and the symmetry of the resolvent, show that this difference is $O(\mu^{-1})$ in maximum-entry norm.

Let Π be the spectral projection of X onto the eigenvalues inside Γ. Cauchy's integral formula now gives

$$g(X)\Pi - g(D_0) = \frac{1}{2\pi \mathrm{i}} \int_\Gamma g(z) \{(z I_n - X)^{-1} - \mathcal{R}_0(z)\} \, \mathrm{d}z,$$

whose maximum-entry norm is $O(\mu^{-1})$. The remaining eigenvalues are at least $a\mu/2 - M$, and $g(t) = 1/(\sqrt{1+t^2} + t) = O(t^{-1})$ as $t \to \infty$. Thus $\|g(X)(I_n - \Pi)\|_2 = O(\mu^{-1})$, proving

$$\|g(X) - g(D_0)\|_{\max} = O(\mu^{-1})$$

for both $X = B$ and $X = \tilde{B}$.

For $f(x) = x + \sqrt{1 + x^2} = 2x + g(x)$, it follows that

$$\left\| f(\tilde{B}) - f(B) \right\|_{\max} = O(\mu^{-1}),$$

because $\|T - R\|_{\max} = O(\mu^{-1})$. Originally $A = f(B) = \Delta C \Delta$ satisfies $1 \leq A_{ii} \leq a^{-1/2}$ and

$|A_{ij}| \le \sqrt{A_{ii}A_{jj}} \le a^{-1/2}$. The same diagonal bounds, up to an $O(\mu^{-1})$ perturbation, hold for $\tilde{A} = f(\tilde{B})$. Normalizing each entry by the square root of its two diagonal entries therefore preserves the uniform $O(\mu^{-1})$ error. This proves the proposition, including the $O(n^{-1})$ rate under pervasive factors. □

Extension to an increasing number of factors. The proof uses the bound on r_n only to obtain $\|T_n\|_2 = O(1)$. All subsequent constants are independent of r_n. Thus the same reconstruction bound holds under Assumption 1 with an increasing number of factors whenever the masked precision correction T_n, defined in the proof, has uniformly bounded spectral norm. This is a sufficient condition; entrywise smallness alone is not used to infer a spectral-norm bound.

S7.2 Gaussian plug-in coordinates

Proposition S2 (Common scaling in Gaussian plug-in coordinates)**.** *Let $\hat{C}_n$ be the sample correlation matrix of T independent, identically distributed Gaussian vectors with positive-definite covariance matrix Σ_n. Suppose its population correlation matrix satisfies $\lambda_{\min}(C_n) \ge a > 0$ uniformly in n. As $n, T \to \infty$, assume $n/T \le \bar{\gamma} < 1$ and $\log n = o(T)$. With $c_n = (1 - n/T)^{-1/2}$,*

$$\max_{i \ne j} \big| [B(\hat{C}_n)]_{ij} - c_n [B(C_n)]_{ij} \big| = O_p\big(\sqrt{\log n / T}\big).$$

No factor representation of C_n is required.

Proof. Correlation is invariant to positive diagonal rescaling, so take $\Sigma_n = C_n$. Suppress n, set $K = C^{-1}$ and $e_n = \sqrt{\log n / T}$, and let S be the centered sample covariance with divisor T. Then $TS \sim W_n(C, T-1)$ and is positive definite almost surely eventually. Gaussian concentration and a union bound give

$$\max_i |S_{ii} - 1| = O_p(e_n), \qquad \max_{i \ne j} |\hat{C}_{ij} - C_{ij}| = O_p(e_n).$$

For each pair $J = \{i, j\}$, the principal block $[(TS)^{-1}]_{JJ}$ is the inverse of a two-dimensional Wishart matrix with $\nu = T - n + 1$ degrees of freedom and scale K_{JJ}^{-1} (Muirhead, 1982, Section 3.2). Thus its marginal distribution is that of

$$K_{JJ}^{1/2} (Z_J' Z_J)^{-1} K_{JJ}^{1/2},$$

where Z_J has ν rows of independent standard bivariate normals. Only these marginal tail

bounds are needed; matrices for different pairs need not be independent. Fixed-dimensional Wishart concentration, inversion on a neighborhood of I_2, and a union bound over all pairs give

$$\max_J \left\|(Z_J'Z_J/\nu)^{-1} - I_2\right\|_2 = O_p\big(\sqrt{\log n/\nu}\big).$$

Here the maximum expresses the uniform tail bound under the joint sample law. Since $\|K_{JJ}\|_2 \le a^{-1}$, $\nu \ge (1-\bar\gamma)T$, and $T/\nu = c_n^2 + O(T^{-1})$, it follows that

$$\max_{i,j} |(S^{-1})_{ij} - c_n^2 K_{ij}| = O_p(e_n).$$

Also $\hat K = \hat C^{-1} = D_S^{1/2} S^{-1} D_S^{1/2}$, where $D_S = \mathrm{Diag}(S)$, so the same bound holds with S^{-1} replaced by $\hat K$. Finally write the exact BCP entry as

$$g(x,p,q,r) = \tfrac{1}{2}\{(pq)^{1/4}x - (pq)^{-1/4}r\}.$$

It satisfies $g(x, c^2p, c^2q, c^2r) = c\, g(x,p,q,r)$ and is Lipschitz on $p, q \in [1, L]$, $|x| \le 1$, $|r| \le L$ for each fixed L. Precision diagonals of correlation matrices are at least one, while $c_n^2 \le (1-\bar\gamma)^{-1}$ and $\|K\|_2 \le a^{-1}$. The sample and scaled population arguments therefore lie in such a fixed set with probability tending to one. Combining the uniform bounds and homogeneity proves the result. □

When n/T has a positive limit, the common scale can differ persistently from one. This need not prevent support recovery: under the factor assumption, Corollary 4 applies with $e_n = \sqrt{\log n/T}$ when its threshold conditions hold. The proposition concerns independent Gaussian sampling; it does not supply a universal correction for dependent or heavy-tailed observations.

S7.3 GFT and InvC bounds and counterexample

Let $H_n = \mathrm{Off}(\log C_n)$, following Archakov & Hansen (2021). The following lemma underlies the GFT and LS shrinkage bounds.

Lemma S2 (Entrywise logarithm bound for a diagonal-plus-factor matrix)**.** *Let $V_n = D_n + U_nU_n'$, where $U_n \in \mathbb{R}^{n\times r_n}$ and D_n is diagonal with entries in a fixed interval $[\omega_-, \omega_+] \subset (0,\infty)$ independent of n. Suppose the rows u_i' of U_n have norm at most L, and $g_n := \lambda_{\min}(U_n'U_n) > 0$. Then*

$$\max_{i,j} |[\log V_n - \log D_n]_{ij}| = O(\log(1+g_n)/g_n).$$

Proof. The integral representation of the matrix logarithm and Woodbury's identity give, with $R_t = (D_n + tI_n)^{-1}$,

$$\log V_n - \log D_n = \int_0^\infty R_t U_n (I_{r_n} + U_n' R_t U_n)^{-1} U_n' R_t \, \mathrm{d}t. \tag{S.7}$$

For every pair, the absolute value of the integrand is at most

$$\frac{L^2}{(\omega_- + t)^2} \frac{\omega_+ + t}{\omega_+ + t + g_n} \le \frac{c_1}{(1+t)(1+t+g_n)},$$

where c_1 depends only on ω_-, ω_+, L. Integration yields $c_1 \log(1+g_n)/g_n$, with absolute convergence entrywise. □

Proposition S3 (Uniform GFT shrinkage)**.** *Under Assumption 1,*

$$\max_{i \neq j} |H_{ij,n}| = O(\log(1+\mu_n)/\mu_n).$$

More explicitly,

$$\max_{i \neq j} |H_{ij,n}| \le \frac{1-a}{a} \frac{\log(1+\mu_n)}{\mu_n}.$$

These bounds apply to all pairs, including correlations bounded away from zero.

Proof. Since $\Omega_n^{-1} \preceq a^{-1} I_n$, $\Lambda_n' \Lambda_n \succeq a\mu_n I_{r_n}$. Apply Lemma S2 with $D_n = \Omega_n$, $U_n = \Lambda_n$, and $L = 1$; $\log \Omega_n$ is diagonal. For the explicit bound, set $R_t = (\Omega_n + tI_n)^{-1}$. Since $R_t \succeq \{a/(a+t)\}\Omega_n^{-1}$ and $\|\lambda_i\|^2 \le 1 - a$, the integrand in (S.7) has entries bounded in absolute value by

$$\frac{1-a}{(a+t)^2} \frac{a+t}{a+t+a\mu_n}.$$

Its integral is $(1-a)\log(1+\mu_n)/(a\mu_n)$. □

Vanishing of every coordinate does not by itself preclude support recovery, since a common rescaling leaves their ordering unchanged. The failure in general is that the leading GFT term can have a different zero pattern.

Proposition S4 (Leading GFT term with homogeneous residuals)**.** *Under Assumption 1, suppose $\Omega_n = \omega I_n$ with fixed $0 < \omega < 1$ and $\mu_n \ge \kappa n$. Set $G_n = \Lambda_n' \Lambda_n$ and $Q_n = G_n/n$. Uniformly for $i \neq j$,*

$$H_{ij,n} = \lambda_{i,n}' G_n^{-1} \log(I_{r_n} + G_n/\omega) \lambda_{j,n} \tag{S.8}$$

$$= \frac{\log n}{n} \lambda_{i,n}' Q_n^{-1} \lambda_{j,n} + O(n^{-1}). \tag{S.9}$$

Proof. Spectral calculus gives $\log C_n = (\log\omega)I_n + \Lambda_n G_n^{-1}\log(I_{r_n} + G_n/\omega)\Lambda_n'$. The eigenvalues of Q_n are bounded above by $\mathrm{tr}(G_n)/n \le 1$ and below by $\omega\kappa$. Thus $\log(I_{r_n} + nQ_n/\omega) = (\log n)I_{r_n} + O(1)$ in operator norm, which proves (S.9) using bounded loading rows. □

Example S1 (Failure of common-threshold separation for GFT and InvC)**.** Let $n = 4m + 3$, $\Omega_n = \frac{1}{2}I_n$, and take the first three loading rows as

$$\lambda_1 = 2^{-1/2}(1,0)', \quad \lambda_2 = 2^{-1/2}(0,1)', \quad \lambda_3 = 10^{-1/2}(1,2)'.$$

Add $3m$ rows $(1/2, 1/2)$ and m rows $(1/2, -1/2)$. All row norms squared equal $1/2$, and

$$G_n = nQ + O(1), \qquad Q = \begin{pmatrix} 1/4 & 1/8 \\ 1/8 & 1/4 \end{pmatrix}, \qquad Q^{-1} = \begin{pmatrix} 16/3 & -8/3 \\ -8/3 & 16/3 \end{pmatrix}.$$

The eigenvalues of Q are $3/8$ and $1/8$, so the factor assumptions hold. Direct calculation gives $C_{12,n} = 0$ and $C_{13,n} = 1/(2\sqrt{5})$, while (S.8) and Woodbury's identity give

$$H_{12,n} \sim -\frac{4}{3}\frac{\log n}{n}, \qquad nH_{13,n} \to \frac{2\log 3}{\sqrt{5}},$$
$$K_{12,n} = \frac{8}{3n} + O(n^{-2}), \qquad K_{13,n} = O(n^{-2}).$$

Indeed, $\lambda_1' Q^{-1}\lambda_2 = -4/3$ and $\lambda_1' Q^{-1}\lambda_3 = 0$. The next GFT term is $\lambda_1' Q^{-1}\log(2Q)\lambda_3/n = 2\log 3/(n\sqrt{5})$, and $K_{ij,n} = -2\lambda_i' Q^{-1}\lambda_j/n + O(n^{-2})$. In both coordinate systems, a common magnitude threshold retaining the nonnull pair $(1,3)$ therefore also retains the null pair $(1,2)$, even after common rescaling. The finitely many loading types have a fixed positive minimum nonzero correlation.

For completeness, InvC's $O(\mu_n^{-1})$ shrinkage follows directly from (S.6).

S7.4 LS bounds and counterexample

Use S_n and D_n defined in Section 7.5 of the main paper. Equivalently, $D_n = \mathrm{diag}(x)$ with $C_n x = x^{-1}$ componentwise. The transformed matrix has zero row sums, and its inverse is $\mathrm{Cor}(e^{S_n})$.

Proposition S5 (LS shrinkage with comparable scaling factors)**.** *Suppose Assumption 1 holds and*

$$\sup_n \frac{\max_i (D_n)_{ii}}{\min_i (D_n)_{ii}} < \infty. \tag{S.10}$$

Then $\max_{i\neq j}|S_{ij,n}| = O(\log(1+\mu_n)/\mu_n)$*, including at fixed nonzero correlations.*

Proof. Let $x_{\min} = \min_i x_i$ and $\tilde{D}_n = D_n / x_{\min}$. The entries of $\tilde{D}_n$ lie in $[1, L]$ for a fixed L. The matrix

$$\tilde{D}_n C_n \tilde{D}_n = \tilde{D}_n \Omega_n \tilde{D}_n + (\tilde{D}_n \Lambda_n)(\tilde{D}_n \Lambda_n)'$$

satisfies Lemma S2, with residual diagonal in $[a, L^2]$, bounded loading rows, and loading Gram matrix at least $\Lambda_n' \Lambda_n \succeq a \mu_n I_{r_n}$. The scalar rescaling contributes only $2(\log x_{\min}) I_n$ to the logarithm, which has no off-diagonal entries. □

Condition (S.10) is sufficient, not necessary. It is not implied by Assumption 1, and the next example shows why no uniform LS sparsity guarantee follows from the original assumptions alone.

Example S2 (LS fills a null pair and shrinks a nonnull pair)**.** Let $n = 8m + 4$, $\Omega_n = \frac{1}{2} I_n$, and $s = 1/\sqrt{2}$. Take the first four loading rows as $(0, s, 0), (0, 0, s), (0, -s, 0), (0, 0, -s)$, followed by $3m$ copies each of $(1/2, s/2, s/2)$ and $(1/2, -s/2, -s/2)$, and m copies each of $(1/2, s/2, -s/2)$ and $(1/2, -s/2, s/2)$. All row norms squared equal $1/2$. The loading Gram eigenvalues are $2m$, $1 + 3m/2$, and $1 + m/2$, so the factor assumptions hold.

Here $C_{12,n} = 0$ and direct substitution into $D_n C_n D_n \iota_n = \iota_n$ gives

$$D_n = \operatorname{diag}\{\sqrt{2} I_4, (2m + 1/2)^{-1/2} I_{8m}\}.$$

Set $\epsilon_m = (4m + 1)^{-1}$, $t_{+,m} = 3m/(4m + 1)$, and $t_{-,m} = m/(4m + 1)$. Rotating the special-variable contrasts $(e_1 - e_3)/\sqrt{2}, (e_2 - e_4)/\sqrt{2}$ to their sum and difference, and pairing them with the corresponding normalized bulk contrasts, reduces the relevant scaled covariance to

$$K_{\pm,m} = \begin{pmatrix} 3 & \sqrt{2t_{\pm,m}} \\ \sqrt{2t_{\pm,m}} & t_{\pm,m} + \epsilon_m \end{pmatrix}.$$

The special-variable sums have eigenvalue one. Consequently, with $f(t) = [\log \left(\begin{smallmatrix} 3 & \sqrt{2t} \\ \sqrt{2t} & t \end{smallmatrix} \right)]_{11}$,

$$S_{12,n} = \tfrac{1}{4}\{[\log K_{+,m}]_{11} - [\log K_{-,m}]_{11}\} \to \tfrac{1}{4}\{f(3/4) - f(1/4)\} < 0.$$

The strict inequality follows analytically from the resolvent derivative

$$f'(t) = -\int_0^\infty \frac{2z}{\{t(1 + z) + z(3 + z)\}^2} \, \mathrm{d}z < 0.$$

For two distinct variables in the first bulk group, $C_{56,n} = 1/2$. Let J contain the eight normalized group indicators and $A_8 = J' D_n C_n D_n J$. Block functional calculus gives $S_{56,n} = \{[\log A_8]_{55} - \log \epsilon_m\}/(3m) = O(\log n / n)$: the scaled residual variances are at least ϵ_m, and

both the scaled residual diagonal and loading Gram matrix are uniformly bounded. Thus $S_{56,n} \to 0$ while the null-pair coordinate has a nonzero limit. No common magnitude threshold separates the two, although the finitely many loading types have nonzero correlations bounded away from zero.

S7.5 Finite-dimensional qualifications

Remark S2 (Dimension alone is insufficient). By (52), at a correlation zero $B_{ij} = 0$ if and only if $K_{ij} = 0$. The positive-definite sequence

$$C_n = \begin{pmatrix} 1 & 0 & 1/2 \\ 0 & 1 & 1/2 \\ 1/2 & 1/2 & 1 \end{pmatrix} \oplus I_{n-3}$$

has $C_{12,n} = 0$ but $B_{12,n} = -1/(2\sqrt{6})$ for every n. Its smallest eigenvalue is $1 - 1/\sqrt{2} > 0$; increasing dimension and a lower eigenvalue bound alone therefore do not ensure preservation.

The partial-correlation row of Table 1 concerns marginal support. To see the distinction, take loading rows $(1/\sqrt{2}, 0), (0, 1/\sqrt{2}), (1/2, 1/2), (\eta, 0)$ with $0 < \eta < 2/7$, and residual variances giving unit diagonals. Then $C_{12} = 0$ but $\rho_{12|3} = -1/7$, whereas $C_{34} = \eta/2 < 1/7$. In a sequential parametrization with variable 3 first, both are coordinates. Adding positive proportions of the two coordinate loading directions makes the factors pervasive without altering these values. No common threshold, before or after Fisher's scalar transformation, retains the latter coordinate while excluding the former.

S8 Empirical implementation and inverse diagnostics

Data and sample construction. We match CRSP daily returns for all available tickers in 2011–2025 to Compustat eight-digit GICS subindustry codes (`gsubind`), retaining all matched observations. Securities are identified by PERMNO, without issuer aggregation or additional exchange, share-type, capitalization, price, volume, or index-membership screens. The return is CRSP's `DlyRetx`, a price return excluding dividends, in decimal units; the risk-free rate is not subtracted. The FF5 and momentum predictors are matched by date and converted from percentages to decimals; `Mkt-RF` is the market predictor.

Of 8,670 securities, 1,765 have finite returns on all 3,772 dates from January 3, 2011 to December 31, 2025. No returns are imputed or winsorized. The 911 duplicate PERMNO–date records in the candidate balanced panel are collapsed after checking agreement of returns,

factors, and classification fields; no conflicts occur. The figures use final available GICS subindustry codes, with ticker and PERMNO breaking ties.

Volatility standardization and inference. Each full-period FF5-plus-momentum OLS regression includes an intercept. The zero-mean GJR-GARCH(1,1) fit uses Gaussian quasi-maximum likelihood, residuals multiplied by 100 for numerical scaling, and an exponentially weighted backcast with decay 0.94 over the first 75 observations. Variances are subsequently restored to return units. The restrictions are $\omega_i > 0$, $\alpha_i \geq 0$, $\alpha_i + \gamma_i \geq 0$, $\beta_i \geq 0$, and $\alpha_i + \gamma_i/2 + \beta_i \leq 1 - 10^{-6}$. Fitted residuals and variances are denoted u_{it} and h_{it}, and $z_{it} = u_{it}/\sqrt{h_{it}}$. For the Gaussian working scores, the shocks are centered and scaled using second moments with divisor T. Bartlett HAC tests use nine lags and the same normalization, treating OLS and volatility filters as fixed; first-stage parameter uncertainty is not propagated. BIC counts the retained correlation coordinates, with those filters common to all columns.

Restricted inverse maps. The common 5% mask leaves retained off-diagonal coordinates unchanged; no maximum-likelihood refit is performed. BCP uses its explicit inverse. For restricted GFT coordinates H, the diagonal iteration is $v \leftarrow v - \log\{\mathrm{diag}[\exp(H + \mathrm{diag}(v))]\}$, initialized at the diagonal of $\log \hat{C}$. It converges in 64 iterations to a maximum absolute log-diagonal error of 9.45×10^{-13}. For LS, reset the diagonal to minus the off-diagonal row sums before exponentiation and correlation normalization. The InvC Newton scheme in Section S6 attains a maximum unit-diagonal error of 5.84×10^{-14}. All four reconstructed matrices are positive definite, and the maximum absolute coordinate recovery error is below 4×10^{-12}.